UNIVERSITY
OF TASMANIA

THE BEHAVIOUR OF CFRP STRENGTHENED STEEL JOINTS

by

HAI BANG PHAN

B. Eng.

Thesis

Submitted in fulfilment of the

requirements for the degree of

Master of Engineering

School of Engineering and ICT

University of Tasmania

August 2015

Statements by the Author

Declaration of Originality

This thesis contains no material which has been accepted for a degree or diploma by the University or any other institution, except by way of background information and duly acknowledged in the thesis, and to the best of my knowledge and belief no material previously published or written by another person except where due acknowledgement is made in the text of the thesis, nor does the thesis contain any material that infringes copyright.

Authority of Access

This thesis may be made available for loan and limited copying and communication in accordance with the Copyright Act 1968.

Statement relating published work contained in the thesis

The publishers of the papers comprising Chapters 3 to 6 hold the copyright for that content, and access to the material should be sought from the respective journals. The remaining non published content of the thesis may be made available for loan and limited copying and communication in accordance with the Copyright Act 1968.

Hai Bang Phan

Statement of Co-Authorship

The following people and institutions contributed to the publication of work undertaken as part of this thesis:

Hai Bang Phan: Candidate (School of Engineering & ICT, University of Tasmania)

Hui Jiao: Author 1 (School of Engineering & ICT, University of Tasmania)

Damien Holloway: Author 2 (School of Engineering & ICT, University of Tasmania)

Chris Taylor: Author 3 (School of Engineering & ICT, University of Tasmania)

Xiao-Ling Zhao: Author 4 (Department of Civil Engineering, Monash University)

The candidate was responsible for the experimental practice, data analyses and manuscript preparation in consultation with supervisors and a honour student.

Author details and their roles:

Chapter 3: Taylor, C., Jiao, H., Phan, H. B. & Zhao, X.-L. (2014). Bond Strength of Steel plates Connected using Strand CFRP Sheets and Selected Epoxy Resins. The 7th International Conference on FRP Composites in Civil Engineering, International Institute for FRP in Construction, 2014 Vancouver, Canada.

This paper has been published.

The candidate and **Author 3** prepared the specimens and analysed data. **Author 1** contributed towards the conceptual design and testing of the specimens and reviewing the results. **Author 4** provided technical consultation and presented the paper in the conference.

Chapter 4: Jiao, H., Phan, H. B. & Zhao, X.-L. 2014. Fatigue behaviour of Steel elements strengthened with strand CFRP sheets. *Advances in Structural Engineering,* 17**,** 1719-1727.

This paper has been published.

The candidate and **Author 1** were responsible for conducting the experiments and analysed the data. Author 1 also contributed towards the conceptual design. **Author 4** provided technical consultation and suggestions about this study.

Chapter 5: Phan, H. B., Holloway, D. S. & Jiao, H. 2015. An investigation into the effect of roughness conditions and materials on bond strength of CFRP/steel double strap joints. *Australian Journal of Structural Engineering*.

This paper was accepted for publication.

Chapter 6: Phan, H.B., Holloway, D.S. & Jiao, H. 2015. The behaviour of CFRP/steel double strap joints in axial tension - A finite element study. *Australian Journal of Structural Engineering*.

This paper is under review.

In chapter 5 and 6, the candidate was responsible for preparing the specimens, testing and analysing the data. The candidate performed FE analysis and compared the theoretical and experimental results. The **Author 1 and 2** contributed towards the conceptual design of the experiments and made suggestions on the experimental testing and theoretical analysis, and also commented and reviewed the reports.

We the undersigned agree with the above stated "proportion of work undertaken" for each of the above published (or submitted) peer-reviewed manuscripts contributing to this thesis:

Hui Jiao

Supervisor

School Of Engineering and ICT

University of Tasmania

Date: 12 Aug. 15

Andrew Chan

Head of School

School of Engineering and ICT

University of Tasmania

Date: 12 Aug 2015

ABSTRACT

In recent years, carbon fibre reinforced polymers (CFRP) have been growing in popularity for external strengthening and repairing of deteriorated steel structures. On one hand, compared to traditional strengthening methods such as welding and bolting, CFRP has shown significant advantages such as light weight, high strength, and corrosion resistance. Furthermore, the application process for CFRP is very simple, quick and requires minimal labour. On the other hand, due to the high strength properties of steel and CFRP, failure is most likely to occur at the bond interface. Therefore, it is vital to study the bond behaviour and the failure mechanism of CFRP strengthened steel structures as well as the factors that play crucial roles in the bond quality. These factors including the material properties, the surface treatment prior bonding or the bond length must be studied before applying in a real structure.

The current research program studied the bond behaviour of double strap joints which were formed by using CFRP to connect two steel plates. Experiment was conducted to investigate the effect of various material properties, bond lengths and surface roughness levels on the bond quality and the failure modes. It was found that there existed an effective bond length for CFRP-to-steel structures; once it was exceeded no improvement in the load carrying capacity could be obtained. This effective bond length varied with material properties, especially the steel grade. It was also found that variations of surface roughness level between 0.73μm and 7.75μm had no significant effect on the ultimate loading capacity of the specimens. However, the CFRP and the adhesive types played very important roles in the bond strength and the failure modes.

Experiments were also conducted to study the fatigue behaviour of double strap joints. These joints were prepared by using strand CFRP with and without primer resin. After the curing process the joints were subject to fatigue tensile loading until failure. The fatigue lives and

failure modes were recorded. Results showed that the fatigue lives of the double strap joints prepared with strand CFRP were comparable to those of specimens strengthened with CFRP plates and other high modulus CFRP sheets. However, a reduction in fatigue life was observed for the samples with primer resin.

A cohesion zone finite element model was established to simulate the bond behaviour and to investigate some factors that could affect the load carrying capacity of the joints such as the steel grade. The results obtained from the model were compared with the experimental data in order to verify the cohesion zone model. The results showed an agreement between the experiments and numerical analysis. The cohesion zone was proved to be suitable for predicting the ultimate load of the joints as well as the stress transfer from CFRP-to-steel. It was found that the steel grade had a significant effect on the bond capacity and the effective bond length.

CONTENTS

ACKNOWLEDGEMENT

I would like to thank my supervisors for their invaluable guidance and support throughout my time at University of Tasmania. **Dr. Hui Jiao,** I thank you for your advice, encouragement and enthusiasm, and giving me a great opportunity to work and widen my knowledge on such an interesting application of carbon fibres. **Dr. Damien Holloway,** I am deeply appreciated for your positivity, advice and editing skills, and I am very amazed at your depth of knowledge in the composite materials.

Mr. Michael Calvert, thank you for your precious time editing my papers, correcting my English, and providing me opportunity to work as an engineer. Our conversations really reduced my stresses and kept me going forwards.

I am extremely grateful to **Mr. Chris Taylor** for his assistance at the early stage of the project.

A big thank you to the technical staffs, **Mr. Andrew Bylett** and **Mr. Peter Seward,** thank you for your kind assistance throughout my Masters.

My **Mum and Dad:** thank you for your love, support and encouragement during the tough times.

Chapter 1. INTRODUCTION

1.1. Background

A large number of steel structures all over the world have been rapidly deteriorating, especially steel bridges. Due to the significant increase in population and the increase in traffic, steel bridges have to carry more loads with higher frequency than before. It is necessary to upgrade or strengthen these structures to meet the current requirements such as higher speed limits or higher load carrying capacities. The demolishing and rebuilding a steel structure is often expensive, time-consuming and inconvenient. Moreover, some structures have significant historic and cultural heritage so that most of steel members must be retained. Therefore it is needed to find a suitable method to strengthen and rehabilitate these structures with low cost, time efficiency and convenience.

Many methods can be used to strengthen steel members such as welding, fastener and rivet joints. These conventional methods have many disadvantages. Firstly, the addition of extra steel plates may lead to the increase in the total self-weight of the entire structure. The added weight makes other steel members carry more loads, thus reduce the efficiency of the structures. Secondly, the heating and cooling involved in the welding process may cause some serious problems related to the lifespan of the steel structures. The stresses and fatigue strength are the key factors that determine the lifespan of structures such as bridges. The welding process causes a reduction in the fatigue strength due to the increase in residual stresses. Additional stresses may also occur because of the distortion caused by welding. Furthermore, it is very difficult to detect any imperfection in a welded joint such as the presence of internal air bubbles and slag inclusion. Thirdly, using rivets can cause some problems for maintenance. The rivets cannot be disassembled so that over time they can become rusty and the only way to replace them is to drill out the existing rivets. Although they can be protected against the weather by coating with a sealant, the cost is high and the

process is more complicated. Finally, using traditional methods for strengthening steel bridges requires heavy equipment to transport and install the materials. The interruption to traffic during the rehabilitation process is inevitable.

In recent years, the conventional strengthening methods have been replaced in many structures by using composite materials such as carbon fibre reinforced polymers (CFRP) or glass fibre reinforced polymers (GFRP). Although carbon fibre was initially utilised in the aerospace industry in the early 1960's and then in concrete structures, the growth of CFRP in the steel industry has been increasing significantly. CFRP has excellent properties that are suitable for strengthening steel structures. These include high tensile strength and elastic modulus, low weight, corrosion resistance and excellent fatigue properties. Moreover, the application process for CFRP does not require heavy equipment, and has low labour demands. With these advantages, the utilisation of CFRP in rehabilitation of steel bridges can solve those issues that were mentioned earlier.

The rehabilitation of Delaware Bridge 1-704 in the United States (Mertz et al., 2002), and the Hythe and Slattocks Bridges in the UK (Luke and Consulting, 2001) are pioneering examples of the use of CFRP in strengthening of steel structures. They are evidence of its viability and cost effectiveness compared with traditional rehabilitation methods such as welding and bolting. However, CFRP-to-steel bonded joints needs to be investigated further due to the lack of knowledge about the durability and bond behaviour of the joints. For instance, strengthening steel structures with CFRP woven sheets may be unpredictable due to the impregnation of resin which may cause unintended adhesion defects. On the contrary, the use of CFRP plates can help getting rid of the adhesion defects but introduce high shear stress at the CFRP ends. Strengthening steel structures with CFRP woven sheets may be unpredictable due to the impregnation of resin which may cause unintended adhesion defects. On the contrary, the use of CFRP plates can help getting rid of the adhesion defects but introduce

high shear stress at the CFRP ends. This study concentrated on improving the above research gap by using different types of CFRP and adhesive resins. The influence of material properties, surface treatment prior to bonding and fatigue loading on the behaviour of the bond between CFRP and steel plate were also studied.

1.2. Research objectives

The project aims to study the bond strength and the failure modes of double strap joints under static and fatigue loading. Various types of CFRP, steel and adhesive were tested. A finite element model was also established to compare the results obtained from the experiment. The main objectives of this project are as follows:

- To study the behaviour of strand CFRP strengthened double strap joints under static load with different parameters that could affect the bond strength. These parameters included the CFRP strength, the bond length of the joint, the adhesive properties, the steel grade and the surface preparation.
- To study the behaviour of strand CFRP strengthened double strap joints under fatigue load and compare the results with previous studies.
- To study the bond strength and the effective bond length of the double strap joints using a finite element model with different parameters such as the steel grades and bond lengths. The results are validated against the experimental results.

1.3. Overall research program

Three series of tests and finite element modelling were conducted in this study.

The first series of tests, which are presented in chapter 3, study the bond strength of CFRP/steel double strap joints using strand CFRP sheet and various epoxy resins. Strand CFRP sheets have been used as an alternative to CFRP plates and CFRP woven sheets in strengthening curved surfaces. The main advantages of the strand CFRP against the

conventional CFRP materials are that it is flexible as the CFRP woven sheets but also minimises the adhesion defects. In practice, strand CFRP can be used to strengthen both flat and curved surface effectively, especially for strengthening steel tubes. Figure 1 shows the details of the strand CFRP. The manufacture process and the material properties are mentioned in Chapter 3.

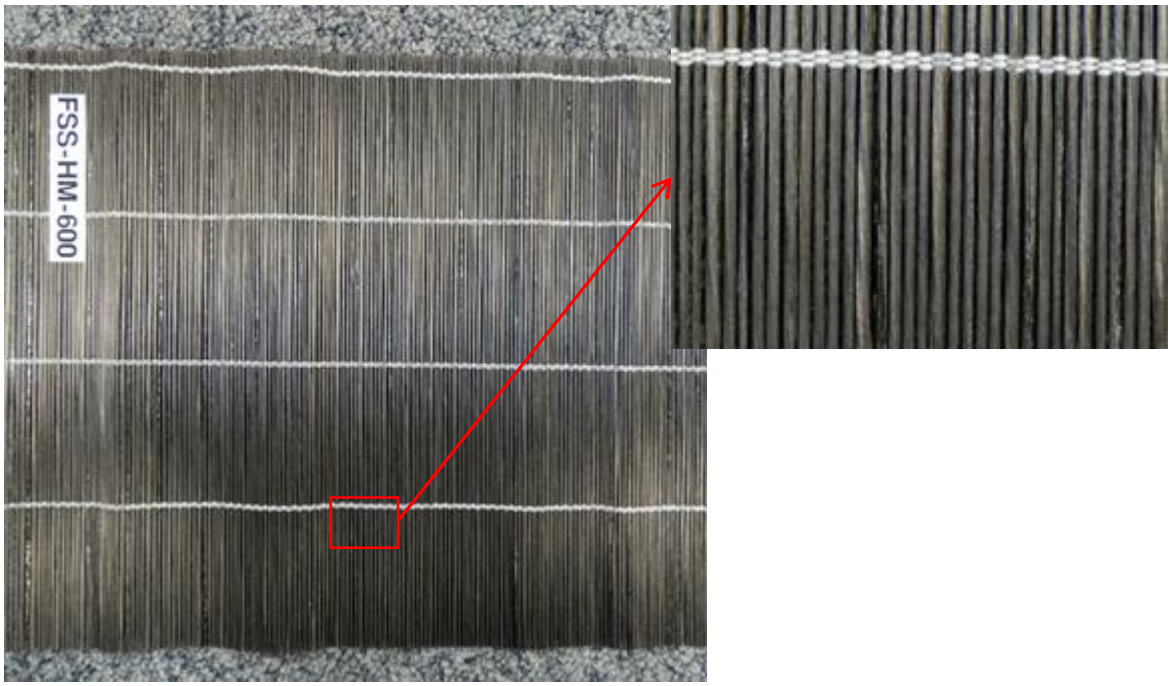

Figure 1. Strand CFRP

However, the bond strength of strand CFRP-to-steel could be affected by the epoxy resins. It was interesting to find out how the bond strength of double strap joints varied with adhesives. Four adhesive resins were investigated in this series: Araldite 420, Nippon, MBrace Saturant and Spabond 345. It was expected that the effective bond length might vary for each type of adhesive so that different bond lengths were adopted in this series. All joints after curing were subject to static tensile load until failure. The ultimate loads and failure modes were recorded. The test results were compared with those reported by other researchers.

The second series of tests, which are presented in chapter 4, study the effect of surface roughness conditions and materials on bond strength of CFRP/steel double strap joints. The bond length was selected based on the effective bond length determined in the first series of tests. Prior to applying CFRP, the steel bonding surface was prepared to create different roughness level ranged from 0.73μm to 7.75μm. Different CFRP materials and steel grades were also investigated. Strain gauges were applied on the CFRP. The tensile load versus strain was recorded for comparison. The surface preparation method was compared with data reported in previous studies. The effect of surface roughness was analysed together with the comparison between bond strength of the samples.

The third series of tests is presented in chapter 5, which study the fatigue behaviour of double strap joints using strand CFRP sheets with or without primer resin. After curing, the samples were subject to fatigue tensile loading. The failure modes and the fatigue lives were recorded for analysis. The results were compared with samples that used different CFRP materials. The study concentrated on the capability of strand CFRP in strengthening steel plates under fatigue loading. Besides that, the effect of primer resin in fatigue loading was also discussed.

The final stage of this study was to perform finite element analysis using ABAQUS. A mixed mode cohesive zone model (CZM) was established with the traction-separation laws of the adhesive through a two-dimensional axisymmetric shell element model. The aim of this part was to compare the results with experimental data such as the effective bond length and the ultimate load. Apart from this the stress transfer mechanism and the shear stress presented at the interface between CFRP and steel were discussed.

Chapter 7 lists the conclusion based on all findings in this study. The chapter also outlines the limitations and identifies future research needs.

Chapter 2. LITERATURE REVIEW

2.1. CFRP material

Carbon fibres are known as high strength, high elastic modulus and low density materials which can be used to mechanically enhance the strength and stiffness of structures. They can be classified based on modulus, strength or heat treatment temperature. In civil engineering application, CFRP is grouped based on its properties (Hegde et al., 2004):

- Ultra high modulus (UHM) with $E > 450$ GPa
- High modulus (HM) with $350 \text{ GPa} \leq E \leq 450$ GPa
- Intermediate modulus (IM) with $200 \text{ GPa} \leq E < 350$ GPa
- Normal modulus and high tensile strength (HT) with $E < 200$ GPa
  and tensile strength > 3 GPa
- Super high tensile strength (SHT) with tensile strength > 4.5 GPa

Carbon fibres were initially used in the military in the 1960s. Since then its application has been increasing significantly. They are now applied in many industries such as aircraft (e.g. aircraft brakes), space structures and construction. According to the estimation from the Composites Market Report in 2014 (Kraus and Kuhnel, 2014), the global demand for carbon fibre will be increased from 31,500 tonnes in 2008 to 89,000 tonnes in 2020. The annual growth rates were expected to be about 10% until 2020 as shown in Figure 2.

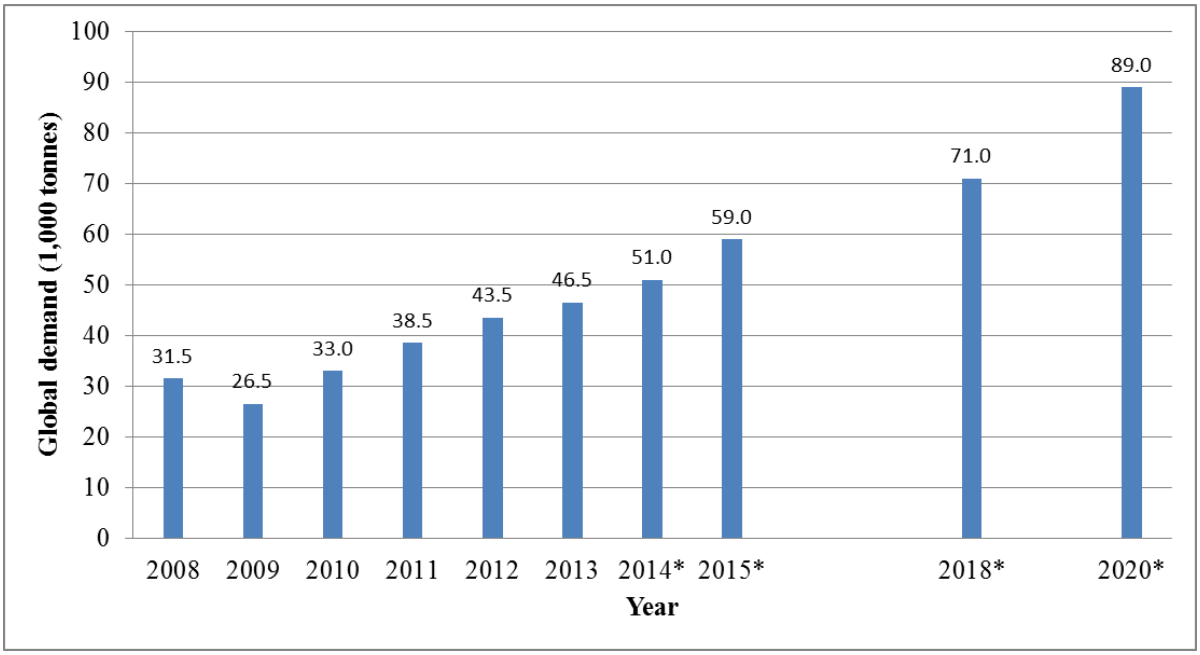

Figure 2. Global demand for carbon fibre from 2008 to 2020 (* estimated) (Kraus and Kuhnel, 2014)

In 2013 there was a remarkable increase in the global demand for CFRP in civil engineering, aerospace & defence and automotive sectors, compared to 2012. In civil engineering the global carbon fibres revenues increased from about $61 million in 2012 $68.5 million in 2013 as shown in Figure 3. This rate has been expected to increase higher in the future due to the manufacturing process becoming simpler and the cost reducing daily.

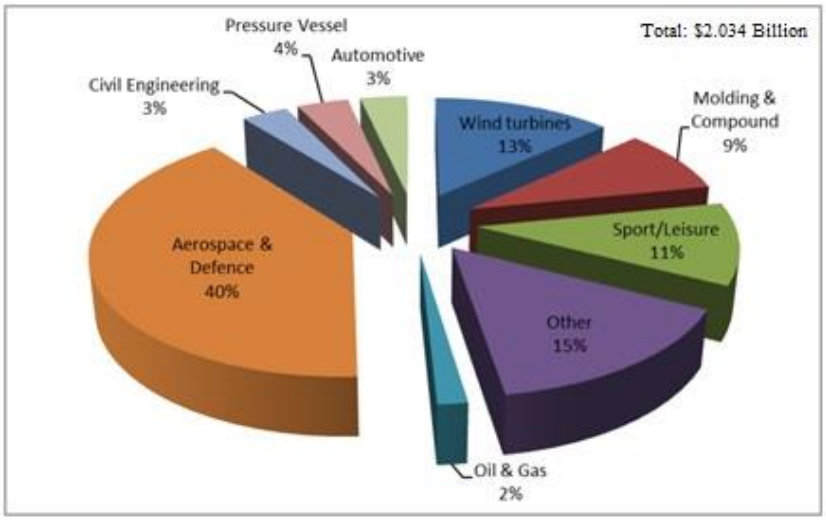

(a)

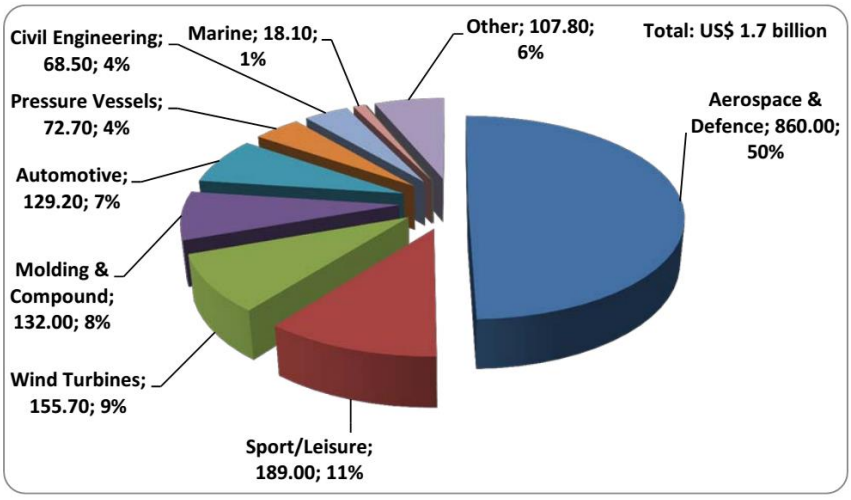

(b)

Figure 3. Global carbon fibres consumption in (a) 2012 and (b) 2013 (Kraus and Kuhnel, 2014) and (Jahn, 2013)

Since CFRP is still a high cost material, its utilisation must be considered carefully. For instance, carbon fibres with ultra-high elastic modulus and thermal conductivity are usually expensive and therefore they are used in critical military and space application. A lower Young's modulus and non-graphitised fibre is much cheaper and used extensively for aircraft brakes (Gorss, 2003).

In civil engineering application, CFRP can be used to strengthen steel or concrete structures via the wet lay-up process which is known as an efficient strengthening method. The common carbon fibre materials that have been using for strengthening purposes are CFRP plate and CFRP woven sheet that are produced by synthetic fibres in a polymeric matrix. Although CFRP plate and CFRP woven sheet are excellent in strengthening steel structures, they must be chosen carefully depending on the situation. Recent studies (Miller et al., 2001, Fawzia and Karim, 2009, Wu et al., 2012a, Bocciarelli et al., 2009) showed that CFRP plate has been completely suitable for strengthening structures with flat surfaces such as the soffit of an I-beam. For uneven surfaces, CFRP woven sheet must be used instead of CFRP plate since it is flexible and can be bent in any direction. However, additional equipment should be used such as a roller to spread the epoxy resin over the fibres and a vacuum pump to take out excessive epoxy resin (Jiao et al., 2012b, Liu et al., 2010). In recent years, CFRP strand

sheets have been introduced in the market. A bunch of individual hardened and continuous fibre strands is connected to form a sheet. CFRP strand sheet was found to be suitable for both curved and flat surfaces and reduced the debonding risk comparing to CFRP woven sheets (Hidekuma et al., 2012). This was introduced as a result of the need to reduce the imperfections during installation as well as reducing the quantity of extra equipment such as roller or vacuum pump. Therefore, strand CFRP is expected to perform as well as CFRP plates and as flexible as CFRP sheets. In this study, both fatigue and static tests are conducted in order to prove this expectation (Chapter 3 and 5).

2.2. Adhesive resin

Adhesive properties play a vital role in influencing the bond strength of steel structures. Recent advances in technology have led to a significant growth in the construction of buildings and bridges thus the use of adhesives in load-bearing joints has also increased. Unlike CFRP-to-concrete structure in which the failure is predominantly by concrete fracture, CFRP-to-steel fails mainly at the adhesive layer. Therefore, adhesive properties play an important role in determining the bond strength of CFRP/steel structures. Bocciarelli and Colombi (2012) and Yu et al. (2012) found that interfacial energy G_f which was associated with adhesive properties was the key parameter affecting the bond strength. The interfacial energy is defined as an area under the bond-slip curve mainly because the double strap joints are symmetric, the peeling stress would be small comparing to the shear stress. Therefore, the peeling forces could be neglected. This energy is absorbed by a chemical linked zone which is known as “toughener” to prevent crack propagation and reduce the brittleness under large peel forces (Mays and Hutchinson, 1992). A typical chemical structure of adhesive resin is shown in Figure 4.

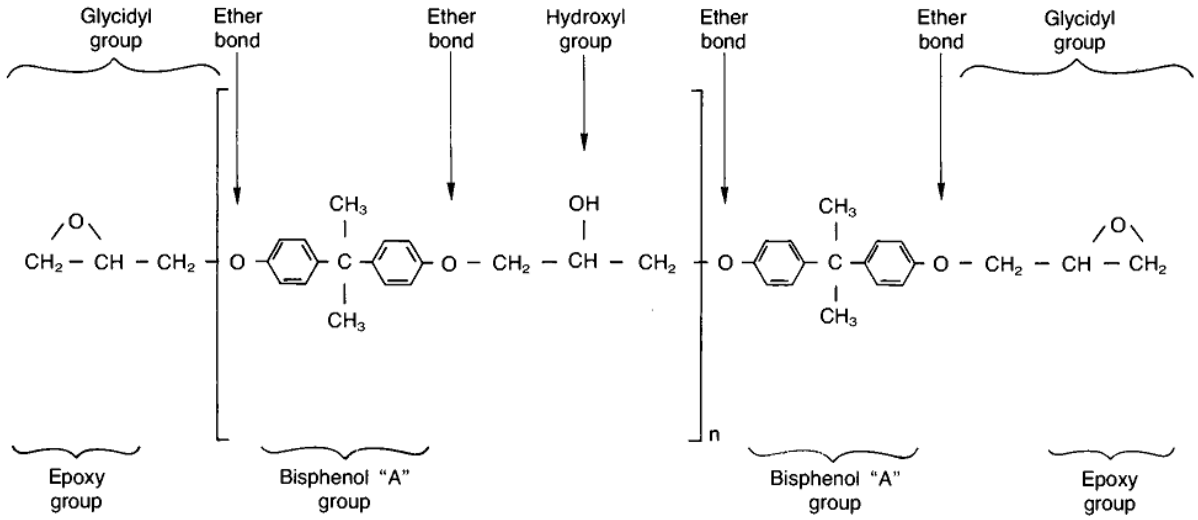

Figure 4. Chemical structure of DGEBA resin (Mays and Hutchinson, 1992)

In order to obtain a good bonding, adhesive resins must be chosen based on certain requirements. These include adequate bond strength, environmental durability, time for curing and ability to prevent galvanic couples formation (Mertz et al., 2002). The bond strength of adhesive is chosen mainly based on its tensile and shear strength, together with the proper surface treatment. However, the bond strength does not depend only on the adhesive, but also on the steel surface treatment. The adhesive resin which is provided by the manufacturer is usually good for bonding with CFRP but not always suitable for steel. Research conducted by Nakazawa (1994) revealed that cold-rolled and galvannealed steel showed better bonding with adhesive than galvanized steel, and adhesive failure was obtained. Therefore, the adhesive type must be suitable for both CFRP and steel.

Other adhesive properties such as strain at failure and Young's modulus are also important and need to be taken in to account. According to Yu et al. (2012), nonlinear adhesives such as Araldite 420 with a large strain at failure and low elastic modulus produced higher interfacial fracture energy, thus improved bond quality. The bond-slip curve for nonlinear adhesive was found to have an approximately trapezoidal shape (Fernando et al., 2014). This bond-slip model could be used to determine the fracture energy which was mentioned earlier. However,

in order to measure the bond-slip relationship, strain gauges must be placed at the adhesive layer, which is extremely difficult. An alternative method of placing strain gauges on top of the CFRP (Yu et al., 2012, Hidekuma et al., 2011, Wu et al., 2010) was used to predict the bond-slip behaviour of a bonded joint.

Due to the difficulty of placing strain gauges at the adhesive layer, some samples presented in this thesis were prepared with the strain gauges applied only on CFRP and then compared with the results obtained by FE model.

2.3. CFRP strengthened steel structures

2.3.1. Surface preparation prior to bonding

Since failure mainly occurs at the steel/adhesive interface, surface preparation for steel is important in creating a strong bond. Existing approaches generally aim to enhance both chemical and mechanical bonding by using tools and chemicals to flatten and clean the surface prior to bonding. These approaches (Baldan, 2004) include:

- To remove all contaminants or pollution on the bonding surfaces to increase surface tension since the contaminants can reduce the contact angle of the adhesive (the ideal contact angle should be zero).
- To increase the roughness of the bonding surface.
- To use chemicals to produce a fresh and stable oxide layer.

Hollaway and Cadei (2002) showed that the weakest link in the metallic joint or FRP/steel joint was the adhesive. This study suggested that before FRP was applied, bonding surfaces must be abraded with a medium sandpaper or a sand blaster followed by cleaning the bonding area with dry cloth and acetone. More generally, Baldan (2004) found that pre-treatment of surfaces could be achieved using (i) physical and/or mechanical, (ii) chemical, (iii) thermal or (iv) plasma method. These methods aimed to ensure a lower surface energy of the adhesive

compared to the adherends. Initially, weak layers such as rust or paint are removed by a physical or mechanical process. A common technique that is used in this process is grit or sand blasting. Poorna Chander et al. (2009) showed that using grit blasting could change the surface roughness depending on the grit size, blasting pressure and blasting time. Furthermore, grit blasting could produce a compressive residual stress on the surface which could help enhancing the bond quality. It was found that there was no difference in bond strength when using different grit sizes (Harris and Beevers, 1999). However, Schnerch (2005) showed that different grit sizes and composition produced different surface profiles. It was recommended that angular, hard grits with minimum Moh's hardness of 6.5 and a minimum specific gravity of 2.65 should be used to obtain good bonding. In the chemical process, a solvent such as acetone was used to remove the contaminants (e.g. grease, oil and water) from the bonding surfaces. An additional technique can also be used before solvent wiping such as use of a vacuum head with brushes (Hollaway and Cadei, 2002).

It is important to apply the adhesive or silane or primer within 24 hours of the surface preparation process in order to minimise a thin oxide layer or recontamination of the bonding surface (Schnerch et al., 2007). Apart from the adoption of applying silane or primer before applying adhesive resin, some studies used phosphate treatments in order to enhance the bond strength and also prevent corrosion within the coating (Sykes, 1982).

In this thesis, some specimens were prepared with primer resin and some were not in order to compare the difference between using and not using primer resin in both static and dynamic loads. Furthermore, since not many studies concentrating on the relation between the roughness and the loading capacity, series 2 of test in Chapter 4 will reveal the effect of the surface treatment (the roughness) on the joint strength.

2.3.2. Bond behaviour and failure modes

Many researchers have studied the bond behaviour and the failure modes of CFRP/steel bonded joints. Generally, five possible failure modes could occur as shown in Figure 5 (Teng et al., 2012b)

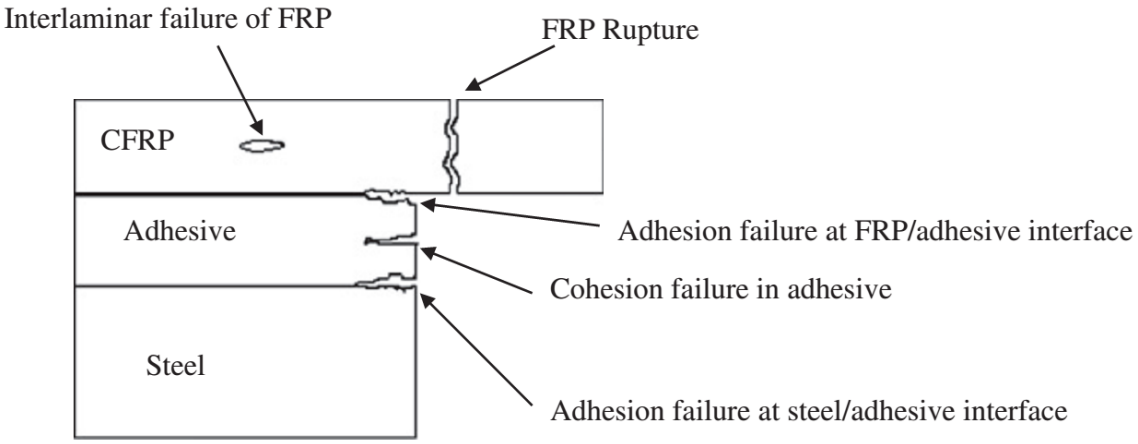

Figure 5. Possible failure modes (Teng et al., 2012b)

Interlaminar failure occurs mainly due to the imperfection while applying the epoxy resin so that the epoxy cannot penetrate into the fibres, or air bubbles are present between the fibres, thus reducing the bonding between CFRP layers. Low viscosity adhesive is recommended so that it can wet all surfaces and fill the gaps between fibres (Teng et al., 2012b). Another method to overcome this problem is to use vacuum bags and rollers. Jiao et al. (2012b) found that air bubbles and excessive epoxy resin could be minimised by using a roller to distribute adhesive evenly over the bonding area and a vacuum bag and vacuum pump to suck out excessive epoxy. This method was found to be effective and hence to improve the bond strength of the joints.

CFRP rupture takes place when the number of CFRP layers is less than the requirement so that the strength of CFRP is less than the bond strength. Therefore, it is vital to consider the number of layers of CFRP before strengthening steel structures. Too many CFRP layers do not help improve the bond strength but cause premature failure due to high stress concentration at the CFRP ends (Hidekuma et al., 2012). Furthermore, according to

Hidekuma et al. (2012) the most effective way was to apply CFRP is with steps in order to reduce the risk of high interfacial shear stress concentration at CFRP tips. The longest layer is in contact with the steel while the shortest layer is the outermost. This study also revealed that the bond strength was improved significantly if the step lamination was applied to only the bottom layer.

The CFRP rupture and the interlaminar failure can be overcome easily so that the adhesion and cohesion failures are most likely to occur. Adhesion failure is mainly due to the low interaction between steel and adhesive while cohesive failure is mainly due to the adhesive properties. From this point of view, cohesive failure is the desired failure mode since the adhesive properties are the main factor related to failure. According to Fernando et al. (2013), grit blasting could be used to generate a surface energy that exceed 50 mJ/m^2 in order to obtain optimum adhesive bond.

The main objective in improving the CFRP strengthening of steel members is to enhance the bond strength, which is defined as the ultimate tensile load of the CFRP/steel member before failure. Many studies have been performed to investigate the bond strength of CFRP/steel structures. Jiao and Zhao (2004b) performed tests involving CFRP strengthened butt-welded circular steel tubes. The steel had an ultimate strength of 1500MPa and a yield stress of 1350MPa. Test results showed a significant increase in strength was achieved when strengthened with CFRP. Although the failure modes between CFRP/steel and CFRP/concrete are different in most of the cases, the bond strength behaviour is quite similar.

The bond strength was found to increase with CFRP bond length, but when the bond length reached a certain value no improvement was achieved in the bond strength (Nozaka et al., 2005, Fernando, 2010, Yu et al., 2012, Teng et al., 2012b). This threshold bond length is referred to as the effective bond length L_e (Teng et al., 2012b). For instance, a series of tests

performed by Miller et al. (2001) indicated that 98% of the forces transfer within 100mm of the bond length. Furthermore, according to the results obtained by Lam (2009), the effective bond length varied from 45mm to 275mm depending on the materials chosen. The effective bond length was also found for CFRP/concrete structures (Athawale, 2012, Ben Ouezdou et al., 2008, Volnyy and Pantelides, 1999). However, a comparison study from showed an incompatibility between strengthening concrete and steel structures by CFRP. This was due to the fact that CFRP with steel bonding was more complicated and the strengthening process was also different.

The above review reveals that adhesion failure is possibly one of the most important. However, the effect of the surface treatment on the joint capacity and the failure mode has not been studied thoroughly. The second series of tests in Chapter 4 will answer this question.

2.3.3. Fatigue behaviour

Fatigue life of steel bridges is one of the most important parameters to determine their service life. In recent years, some researchers have been studying the effects of fatigue loading on the bond strength of CFRP-to-steel structures. Generally, the fatigue loading has a minor influence on the bond joints and the failure modes (Liu et al., 2010, Wu et al., 2013).

Liu et al. (2010) performed a series of tests with double lap joints using normal and high modulus CFRP. The samples were subject to fatigue loads with various loading ratios. The loading ratio was defined as the ratio between the minimum load and the maximum load in one cycle. After a certain number of cycles, the specimens were subject to static tensile test until failure. It was found that fatigue loading with different loading ratios did not affect greatly the ultimate tensile strength of the specimens strengthened with high modulus CFRP. However, for the specimens strengthened with normal modulus CFRP under the fatigue loading ratios between 0.2 and 0.3, the ultimate tensile strength was reduced by up to 20%. The failure modes were found to be similar to those in the static tensile tests. These

observations were confirmed by a later experimental program conducted by Wu et al. (2013). Furthermore, it was concluded that fatigue loading caused a minor reduction in stiffness due to a very small damage region close to the joint.

However, a comparison study between the fatigue life of CFRP-to-steel samples and welded cover plates established by Bocciarelli et al. (2009) showed the contrary. In this experiment, steel plates were strengthened on both sides by CFRP laminates. All samples were subject to fatigue loading with various stress ranges. The failure modes and fatigue life were recorded. A remarkable reduction in stiffness of the samples under fatigue loading was found. The main reason was the progressive debonding of the adhesive. When debonding reached 50% of the bond length, the stiffness reduced to 85% and failure started to take place rapidly.

Apart from the influence of fatigue loading on the bond strength, it is also important to improve the fatigue life of CFRP strengthened steel structures. An experimental program conducted by Jiao et al. (2012a) demonstrated the effects of different strengthening methods on the fatigue life of steel beams with defects. An initial cut was made at the mid-span of the beam to reflect a crack. This crack was strengthened by either CFRP laminates, CFRP woven sheets or welding. It was found that CFRP plate could extend the fatigue life of the specimens by 7 times compared to welding. Additionally, four layers of CFRP woven sheet could also increase the fatigue life about 3 times.

Talreja (1981) established a schematic fatigue life diagram for unidirectional FRP under tensile load as shown in Figure 6. The load was parallel to the fibre direction. In this diagram, strain was chosen since it is an independent variable for both the FRP and matrix. According to Talreja (1981), the fibre breakage occurred randomly due to high stress concentration. The amount of fibre breakage increased with fatigue cycles, causing higher stress concentration at the unbroken fibres.

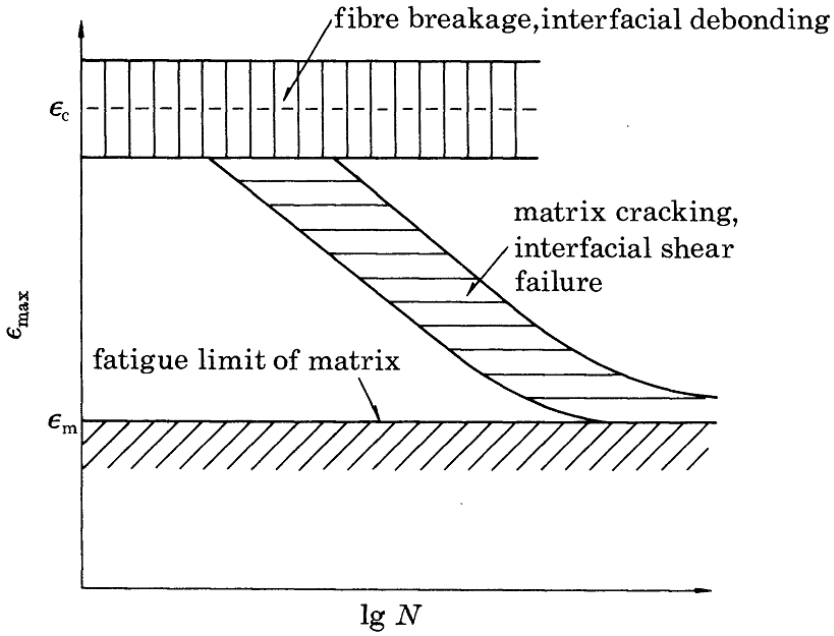

Figure 6. Fatigue life diagram and failure modes (Talreja, 1981)

In order to reduce CFRP debonding under fatigue loads, the selection of CFRP laminate and adhesive properties are extremely important (Bocciarelli et al., 2009). Furthermore, the loading direction must be parallel to the fibre direction. Talreja (1981) found that unidirectional CFRP had the highest fatigue resistance, but if there was any deviation such as the fibres being placed with a small angle from the loading direction it could cause a significant reduction in fatigue life.

Depending on the situation, prestressed CFRP laminates could be considered as an effective method for strengthening. Luke and Consulting (2001) reported the application of prestressed CFRP plates for increasing the loading capacity of historic bridges in the UK. The bridges were initially designed to carry loads of about 7.5 tonnes. Due to some difficulties such as low headroom and low budget, traditional strengthening methods could not be performed. The bridges were strengthened using two 4mm thick CFRP plates with a width of 100mm and a length of 7.5m. After installation, the loading capacity was increased to 40 tonnes (about 533% of the original loading capacity). Furthermore, using CFRP helped the Council save about £20,000 compared to the alternative approaches.

2.3.4. Under severe environments

The environmental durability of CRRP/steel structures depends greatly on adhesive properties. It was found that under extreme temperature environments, the bond strength of CFRP/steel samples reduced significantly (Nguyen et al., 2011). This was due to the glass transition temperature T_g of epoxy resin which was defined as a temperature region where the polymer transfers from a "hard" to a "soft" material. It is noted that a "soft" material is more pliable and compliant than it is at room temperature. An epoxy resin with a high T_g value is recommended for CFRP/steel bonding in regions with high temperature. The T_g value depends strongly on the curing method. The T_g is lower when curing at room temperature and higher when curing at an elevated temperature. Nguyen et al. (2011) found that the glass transition temperature was proportional to the effective bond length; when the temperature was close to the glass transition temperature of an epoxy resin, the effective bond length increased nearly twice that of the bond length at room temperature. Although the strength of the CFRP materials did not change when the temperature was close to or above the adhesive T_g value, the ultimate tensile strength and stiffness of specimens were reduced dramatically, by about 20% at the T_g temperature and up to 80% at 20^{o}C above the T_g value. Since the adhesive changes its properties at the T_g temperature, when the temperature reached T_g or above T_g, failure would occur at the adhesive layer due to the reduction in shear strength of the adhesive. Therefore, it would be recommended that the bond length of CFRP-to-steel should be larger than the effective bond length to reduce the risk at elevated temperature (Nguyen et al., 2011). In recent years, new adhesives have been introduced with very high T_g values such as the heat resistance resin FB-E9S or heat resistance primer FP-N9. These adhesives showed excellent temperature resistance up to 78^{0}C (Hidekuma et al., 2013).

Another issue related to the environmental durability of CFRP/steel structure is galvanic corrosion which is known as an electrochemical process when coupled metals are in contact

with an electrolyte. Some common environments that galvanic corrosion could occur include: sea water, atmospheric environments (e.g. trapped rainwater or high humidity or polluted regions), buried and embedded metals, oil and gas environments, and acidic and alkaline environments (Francis, 1982). The conditions necessary for galvanic corrosion of CFRP/steel structures are:

- An electrolyte bridging the CFRP and steel.
- A presence of electrical connection between the CFRP and steel.
- A sufficient difference of electrical potential between the CFRP and steel.
- Consumption of dissolved oxygen taking place during sustained cathodic reaction.

CFRP is an electron conductor and is high in the galvanic series. Steel, meanwhile, is highly active and low in the galvanic series. Therefore, when steel and CFRP are in contact in sea water, they are adversely affected and the contact between them can be extremely undesirable. A series of tests conducted by Tavakkolizadeh and Saadatmanesh (2001) showed the existence of galvanic corrosion when CFRP and steel are in direct contact. However, the galvanic corrosion rate depended on the contact level and time of the exposure. For instance, the strength and stiffness of CFRP/steel joints reduced rapidly in the first 2-4 months in sea water (Nguyen et al., 2012). It was recommended that using nonconductive adhesive resin could help to minimised this problem. An alternative method is to pre-treat the bonding surface with silane coupling agent prior bonding. Dawood and Rizkalla (2010) showed that an additional layer of silane or glass fibre reinforced polymers (GFRP) could prevent this phenomenon.

2.4. Numerical and theoretical models

In recent years, many companies have introduced very powerful structural FEA programs in the market such as ABAQUS, ANSYS, COMSOL, etc. These programs have become simpler and easier for users to perform analyse. Numerical analysis is extremely important not only

for confirming experimental results but also for predicting the likelihood of potential flaws and ways to prevent them. Generally, three numerical methods could be exploited: finite element method (FEM), boundary element method (BEM) and finite difference method (FDM). Depending on the available data and the surrounding conditions such as boundary, diffusion or failure behaviour of the structures, a suitable method could be chosen to give the best output. For FRP-to-metal structures, FEM has been proved to be an excellent method for analysis by Mitchell et al. (1975) and Ratwani (1977).

FEM has been developed since the early 1960s and has become a common method that has been used for analysis because of its advantages such as stability, convergence, adaptability and flexibility. In general, FEM is used to divide a very complicated problem into many small elements which are connected at "nodes". These elements can be solved easier in relation to each other with a set of simultaneous algebraic equations. The equation can be expressed as

$$\boldsymbol{Ku} = \boldsymbol{F} \qquad (1)$$

$$Hence \quad \boldsymbol{u} = \boldsymbol{K}^{-1}\boldsymbol{F} \qquad (2)$$

Where **K** is the properties of materials such as stiffness, thermal conductivity, viscosity, etc.

F is the action that is applied on the structures such as force, heat source, etc.

u is the structural behaviours such as displacement, temperature, velocity, etc. In the equations (1) and (2), **u** is usually an unknown and needs to be solved. However, in some problems, **F** and **u** are both unknown. In this case, the relation between the action and behaviour is extremely important. Furthermore, adhesive bonded joints are usually "overdesigned" due to a lack of suitable material models and failure criteria. Care must be taken in order to obtain a good result using FEM (da Silva and Campilho, 2012).

Al-Zubaidy et al. (2013) performed finite element modelling of double strap joints under dynamic loading conditions. In this study, various CFRP layers were applied to strengthened steel plates as shown in Figure 7. The samples were subject to different dynamic loads of 3.35, 4.43 and 5m/s. The ultimate load and effective bond length were recorded for comparison with experimental data. It was found that the results obtained by FEM agreed very well with those obtained in the experiment. However, with a higher number of CFRP layers, the results were slightly different. It was also found that the effective bond length was well predicted by FEM.

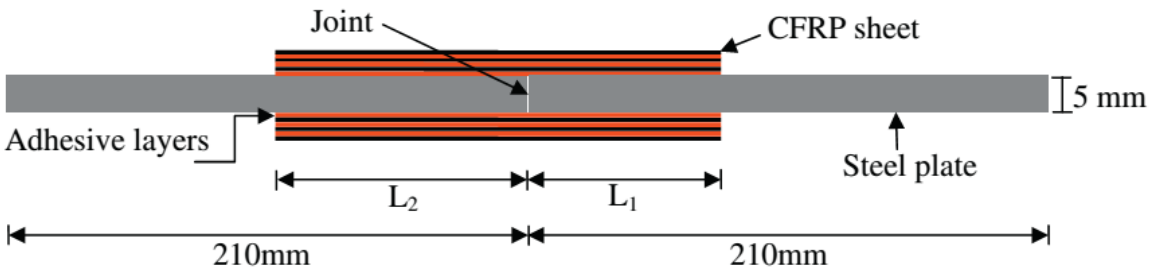

Figure 7. Specimen's geometry (Al-Zubaidy et al.)

Jiao and Zhao (2008) established a three-dimensional model to study the failure progress of CFRP strengthened butt-welded circular steel tubes. Four layers of CFRP sheets were investigated using reduced integration three-dimensional elements. The adhesive layers were modelled using cohesive element with zero thickness based on the traction separation law. It was found that the debonding and the ultimate loads agreed well with those obtained in the experiment.

In this thesis, FE models are presented by applying similar principle as those in Jiao and Zhao (2008) using traction separation law with zero thickness adhesive resin. The results were compared with experimental results.

Taylor, C., Jiao, H., Phan, H. B. & Zhao, X.-L. (2014). Bond strength of steel plates connected using strand CFRP sheets and selected epoxy resins. Proceedings of the 7th International Conference on FRP Composites in Civil Engineering, International Institute for FRP in Construction, 2014 Vancouver, Canada.

Chapter 4. THE EFFECT OF ROUGHNESS CONDITIONS AND MATERIALS ON BOND STRENGTH OF CFRP/STEEL DOUBLE STRAP JOINTS

4.1. Introduction

Recent studies show that CFRP has great advantages in strengthening of degraded steel structures (Teng et al., 2012b, Jiao et al., 2012b, Jiao et al., 2013), particularly due to its high strength to weight ratio and rapid installation time. CFRP was found to be suitable for strengthening of both metal and concrete structures (Teng et al., 2001, Parvin and Brighton, 2014). The rehabilitation of Delaware Bridge 1-704 in the United States (Mertz et al., 2002), and the Hythe and Slattocks Bridges in the UK (Luke and Consulting, 2001) are pioneering examples of the use of CFRP in strengthening of steel structures. They are evidence of its viability and cost effectiveness compared with traditional rehabilitation methods such as welding and bolting.

It continues to be improved due to the significant outcomes from recent applications in Civil Engineering. CFRP strengthening techniques have continued to improve significantly in recent years. Many types of CFRP have been introduced such as CFRP woven sheets, CFRP plates, and CFRP strand sheets, together with various adhesives such as Araldite 420, Sika Sikadur-330, Spabond 345 and one of the newest products, the heat resistant FB-E9S (Hidekuma et al., 2013).

The loading capacity of CFRP reinforced structures depends greatly on the interface bonding of both steel to adhesive and CFRP to adhesive. The interface bonding not only depends on the adhesive itself, but also on the surface energy, roughness and topography. The surface energy is the total energies present on a surface of a loaded solid. It can be also considered as the surface excess energy per unit area of surface. The surface energy is associated with the surface roughness, that is, the change in roughness level causes a change in surface area thus changes the surface energy. Roughening the surface may reduce the contact level between

adherends (Tamai and Aratani, 1972).The surface roughness is the key factor that affects the fracture energy G of the adhesive joint. A rougher surface increases the surface area, thus reduces the surface excess energy ($G_0 = \Delta G/A$). However, Packham (2003) found that a very rough surface might reduce the bonding capacity, and the optimal roughness should range from microns to nanometres in order to enhance the fracture energy.

Generally steel surface treatment can be done by hand grinding, sand or grit blasting. Some researchers showed that sand blasting could create a better surface for bonding than hand grinding (Liu et al., 2010). Fernando et al. (2013) and Teng et al. (2010) showed that the grit blasting process could be used to avoid adhesion failure, so that failure occurred within the adhesive and the bonding capacity then depended only on the adhesive properties. The grit-blasting process can also change the physical and chemical properties of the surface such that it has a significant effect on the bond behaviour (Harris and Beevers, 1999).

There is however limited information available on the effect of surface roughness on the CFRP-adhesive-steel system. The influence of surface roughness was investigated in (Chataigner et al., 2012). Three different surface roughness levels of 7μm, 10μm and 13μm were obtained by sand blasting with different grit sizes and no significant difference was found between the ultimate loads. The failure modes of those samples were also the same.

The aim of this study is to examine the bonding capacity and bond behaviour of CFRP-to-steel specimens with various CFRP forms, adhesives and roughness levels. Two steel plates were connected by a CFRP/adhesive system to form a double strap joint specimen. A total of 25 specimens were prepared with either CFRP woven sheets, strand sheets or plates, with the epoxy resins Sikadur-330, Spabond 345 or Nippon FB_E9S. A range of steel surface roughness from 0.73μm to 7.75μm was generated by using two different grinding discs. This range is more reasonable in reality compared with that of Chataigner's study. On the other

hand, a rougher surface may lead to the difficulty in cleaning the surface. After curing, all specimens were subjected to a static tensile test until failure.

4.2. Material properties

In this study, both mild and high strength steels were investigated, since some difference may be expected in the effective bond length due to the different stress-strain relationships of mild and high strength steels.. A total of 18 mild steel and 7 high strength steel specimens were prepared. Tensile coupon tests in accordance with AS1391 (SAA1991) produced the yield stress and ultimate tensile strength of the steel plates as shown in Table 3.

Table 3. Steel properties

Type of steel	Yield stress (MPa)	Ultimate tensile strength (MPa)	Ultimate strain (%)
Mild steel	350	541	5.18
High strength steel	1100	1362	1.37

Sika, Spabond and Nippon adhesives were used in this study. Some researchers believed that Araldite 420 is the best choice (Liu et al., 2010, Fawzia et al., 2005a, Wu et al., 2012c), however other adhesives have been chosen in this study due to the initial availability. The mechanical properties of each adhesive are shown in Table 4. For the Nippon adhesives, both the primer FP_WE7W and bonding adhesive FB_E9S were used on the same specimens. The main purpose of the primer resin is to prevent direct contact between the CFRP and steel in order to reduce the possibility of galvanic corrosion. Nippon FB_E9S is a heat resistance resin with a glass transition temperature T_g of 78^0C. Nguyen et al. (2011) found that the temperature was proportional to the effective bond length. Since the adhesive changes its properties at temperature T_g, when the temperature exceeded T_g failure would occur at the adhesive layer due to the reduction in shear strength of adhesive. Hidekuma et al. (2013) found for those specimens strengthened by heat resistant adhesives, the failure did not occur

at up to 60°C due to the unchanged properties of adhesives at this temperature. The use of the heat resistant adhesive could solve the temperature issue stated by Nguyen et al. (2011).

Table 4. Properties of adhesives

Type of adhesive	Elastic Modulus (GPa)	Tensile Strength (MPa)	Shear Strength (MPa)
Sikadur-330	4.5	30	15
Spabond 345	2	13	36
Nippon FB_E9S	4	30.7	16
Nippon FP_WE7W	2.2	20.6	20.2

In order to determine which type of CFRP provides better bonding, MBrace Laminate, SikaWrap and Nippon Strand carbon fibres were investigated. The fibres were unidirectional and oriented in the tensile direction. By using various CFRP types the failure modes could be compared and a recommendation could also be made for strengthening. The MBrace Laminate is a hardened CFRP plate with a thickness of 1.4mm, a fibre content of 70% and interlaminar shear strength of 80MPa. The MBrace Laminate can be used only for strengthening flat surfaces. SikaWrap is a woven CFRP sheet that can be used for strengthening both curved and flat surfaces. The CFRP woven sheets are normally applied in multiple layers due to its small thickness of 0.13mm. Nippon Strand is an intermediate CFRP sheet that can be used for flat and developable curved surfaces, such as steel tubes with the fibre direction along the longitudinal axis of the tube. The strand CFRP sheets are formed by tying together impregnated CFRP strands with a diameter of about 1.2mm. Hidekuma et al. (2011) found that no delamination occurred until the steel reached its yield load when strand CFRP was applied. Several layers of strand CFRP can also be employed to strengthen steel structures, but the debonding risk is also higher (Hidekuma et al., 2012). Table 5 shows the properties of each type of CFRP.

Table 5. CFRP properties

Properties	MBrace Laminate	SikaWrap*	Nippon Strand Sheets
Elastic Modulus (GPa)	170	231	690
Tensile Strength (MPa)	3100	4100	3010
Ultimate Strain (%)	1.6	1.7	Not specified

Thickness (mm)	1.4	0.12	1.2
Fibre Areal Weight (g/m^2)	2240	220	630

* The SikaWrap properties were specified by the manufacturer when combined with Sika Sikadur-330 to form a composite. These properties may differ when another epoxy resin is used.

4.3. Specimen preparation

In this study, the double strap joints were formed by connecting two steel plates with the dimensions of 300mm long, 50mm wide and 5mm thick using CFRP and adhesive system as shown in Figure 13. The bond length *L* was the measure from the joint to the CFRP end. Three different bond lengths of 75mm, 100mm and 125mm were adopted for series 1.

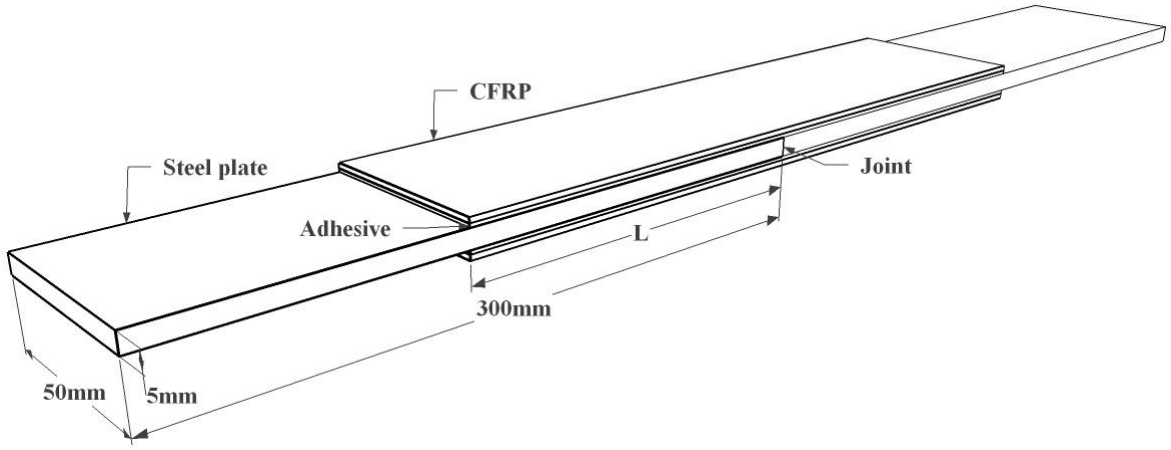

Figure 13. Double strap joint schematic view (not to scale)

The steel plates were ground using either the flap disc FlexOvit Mega-Line Blue or FlexOvit reinforced A24/30T. The purpose of using different grinding discs was to generate a variety of roughness levels. The profile roughness parameter (the arithmetic mean deviation of the profile R_a) ranged from 0.73µm to 7.75µm. After generating the surface roughness to enhance mechanical bonding acetone solvent was used to remove rust, grease, oil and other loose chemical to increase chemical bonding between the adhesive and steel surface. Hollaway and Cadei (2002) believed that using solvent to clean the surface could redistribute dust on the bonding surface. However, El Damatty and Abushagur (2003) showed that the dust could be completely removed by using a large amount of solvent such as acetone. In this study, all specimens were cleaned using acetone solvent. However, for those specimens of high roughness, solvent wiping redistributed dust on the bonding surface due to sharp surface

topography, which could cut the wiping clothes into very fine pieces. An additional step was taken to make sure that the bonding surface was completely clean by using a brand-new paintbrush to remove the remaining dust.

After preparing the steel surface, the roughness was measured using the Mitutoyo Surftest-301. This equipment works well within the temperature range of 5ºC to 40ºC. In order to obtain accurate results, the following environmental conditions must be achieved:

- A testing location is chosen with a flat, firm surface and minimal fluctuation, since vibration can significantly affect measurement results.
- The equipment should be isolated from any electrical noise source.

Key components of Surftest-301 are the main unit, the drive connector and the detector unit as shown in Figure 14. The detector operates on the differential inductance method with a measuring force of 4mN. Its needle is a diamond with the tip radius of $5\mu m$. The unit was calibrated according to the manufacturer's specifications.

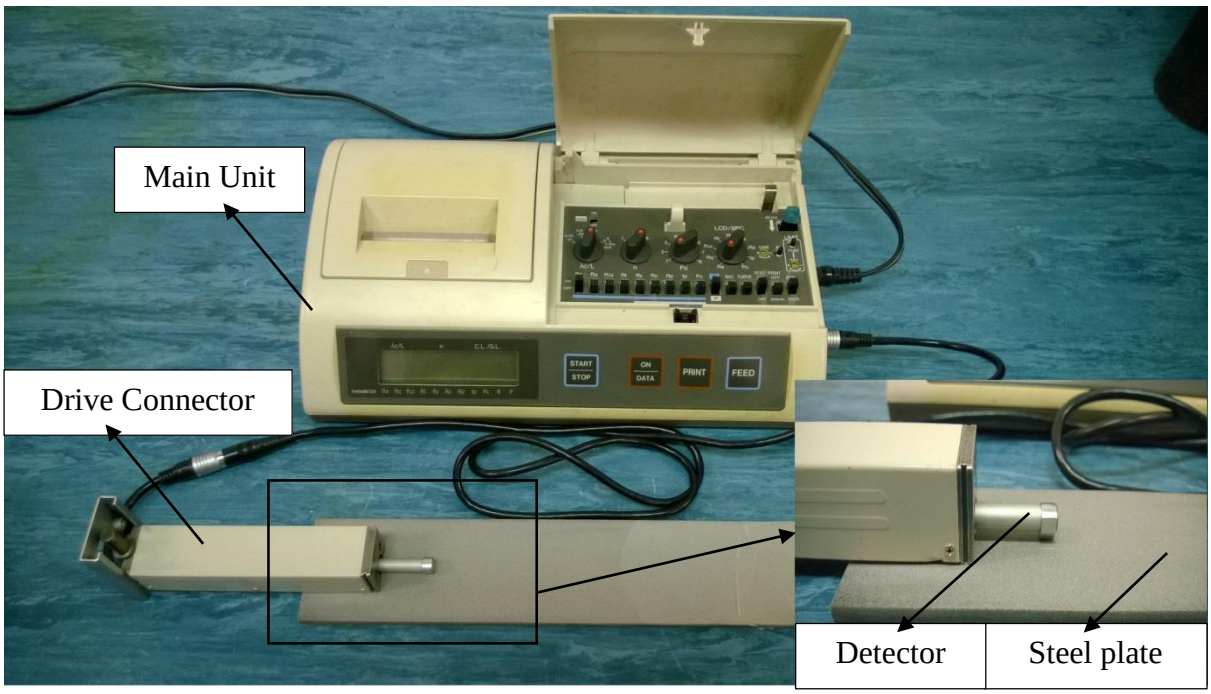

Figure 14. Surftest 301 main parts

The Surftest-301 has an analog filter (2CR) with a detector travel speed of 0.5mm/s – a conventional filter with the traverse length equal to (start-up length) + (evaluation length). The detector starts to record the surface roughness after the start-up length of 1mm and the evaluation length depends on the sampling span setting according to

$$evaluation\ length = \lambda c \times n$$

where: λc is the cutoff value and n is the number of sample spans, which can be set to 1, 3 or 5 as shown in Figure 15.

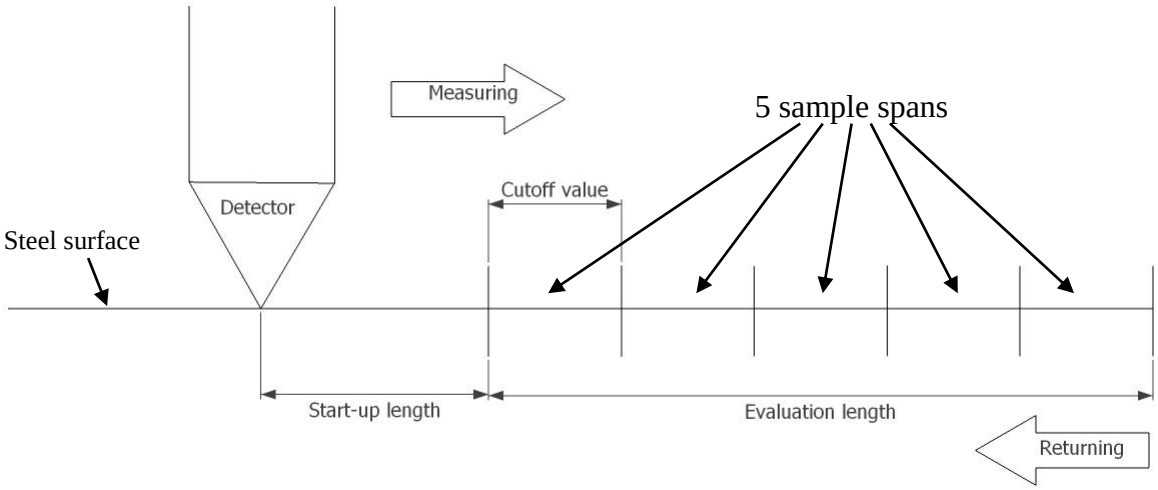

Figure 15. Traverse lengths of the detector

The Surftest-301 is capable of measuring eight measurement parameters. The values of λc and n were set to 2.5mm and 5 respectively. The measuring range for R_a is from 0.05 to 40µm. The measurement was made at about 50 different locations for each sample, then the average value of Ra was calculated. Figure 16 shows the roughness measurement by Surftest-301 and a roughness chart of mild steel prepared with Mega-Line Blue disc.

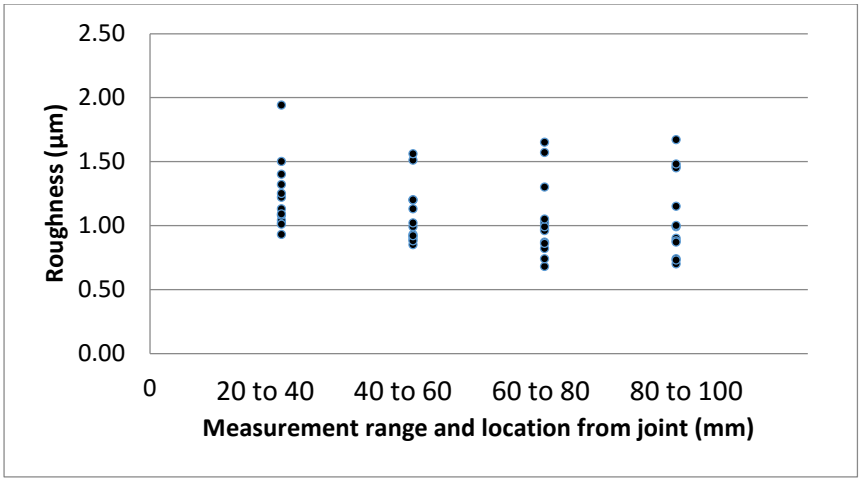

Figure 16. Roughness measurement points of sample HCP1

After surface treatment, the primer/adhesive resin was applied immediately to avoid the formation of any contamination and/or oxidation layer. The resin was applied using a paintbrush to create a uniform thickness. For those specimens prepared with the Nippon adhesive the primer resin was first applied to a thickness of about 0.125mm and cured for one day before applying the bonding resin and CFRP.

The CFRP was then placed in position with a uniform pressure applied on the external surface of the CFRP to bleed out excessive adhesive and air bubbles. The pressure was also intended to create a uniform thickness of adhesive which could affect the bond behaviour. Xia and Teng (2005) showed that the adhesive thickness should be less than 2mm in order to obtain ductile failure. However the adhesive thickness is not the focus of this paper so all series of tests were conducted with approximately 1mm of adhesive thickness. All samples were cured for at least one week before testing.

4.4. Experimental details

4.4.1. Series 1: Effective bond length

An effective bond length is defined as the length of CFRP that can be applied in order to obtain the optimal tensile capacity of the joint. When exceeded, the bond capacity is not improved. The effective bond length varies with type of CFRP and adhesive. Taylor et al. (2014) obtained an effective bond length of 80mm using CFRP strand sheets and Araldite

420, while Liu et al. (2010) found the bond length to be 60mm for double strap joint specimens. However, Miller et al. (2001) showed that 98% of the force was transferred within 100mm of the end of CFRP strips for a particular CFRP/adhesive system. The force transfer length is associated with the geometric and material properties. The adhesive which has a high strain capacity may result in a larger bond length, which will increase the ultimate tensile capacity of the joint. A longer CFRP bond length may be used to increase the ductility of the system, but it will not improve the ultimate load. As CFRP is quite expensive, it is worthwhile determining the effective bond length before studying the effect of roughness on the bonding capacity. In this series of tests six samples were prepared with three different bond lengths, in the range 75 - 125mm as shown in Table 6.

Table 6. Series 1 testing results

Steel	Adhesive	CFRP	Bond Length (mm)	Ultimate Tensile Load (kN)
High strength	Sikadur-330	MBrace Laminate	75	77.5
High strength	Sikadur-330	MBrace Laminate	100	118.5
High strength	Sikadur-330	MBrace Laminate	125	119.0
Mild steel	Sikadur-330	MBrace Laminate	75	70.0
Mild steel	Sikadur-330	MBrace Laminate	100	89.2
Mild steel	Sikadur-330	MBrace Laminate	125	90.1

For those samples prepared with a 125mm bond length, five strain gauges (SG1-5 in Figure 17a) were positioned on one side at equal intervals (approximately 28.75mm) between the bond end and the joint. The main purpose of these strain gauges was to measure the strain behaviour of CFRP at different locations, hence to identify the location of initial failure.

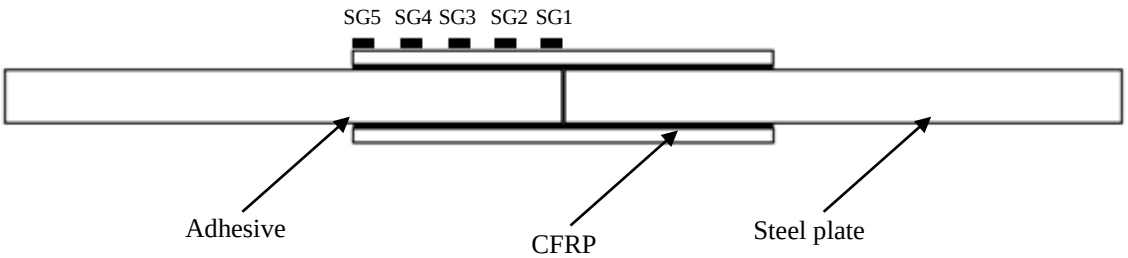

a)

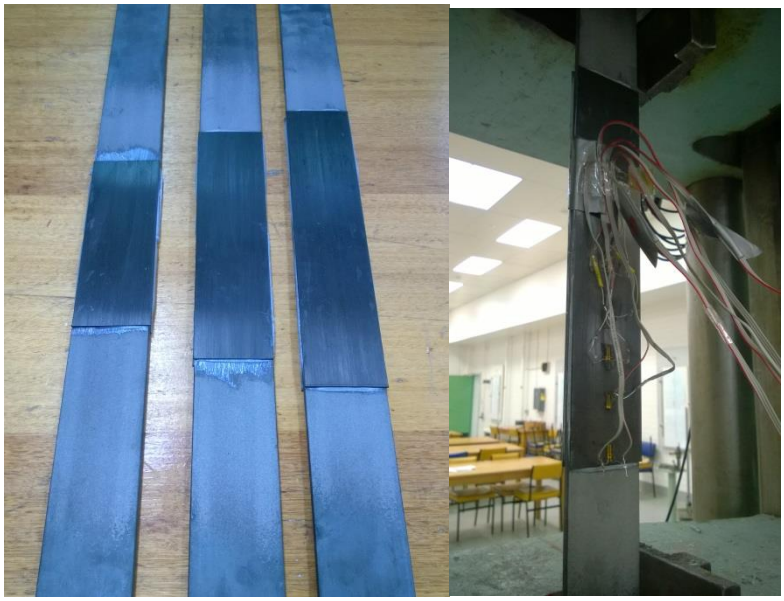

b)

Figure 17. Series 1 testing: a) Side view of the sample with attached five strain gauges. b) samples with different bond lengths

For all samples cohesive failure occurred within the adhesive layer. The ultimate loads were very similar for samples with bond lengths of 100mm and 125mm in both the mild and high strength steel specimens, suggesting that the bond length required to develop full load was between 75mm and 100mm. The longer the bond length was, the more ductile was the specimen. Hereafter, a single bond length of 100mm was adopted for series two and three tests.

4.5. Series 2: Influence of surface roughness on the joint strength

In this series a total of eight specimens were prepared with different surface roughness. Their roughness values, ultimate tensile loads and failure modes are presented in Table 7. After curing, all samples were tested until failure using an Avery Universal Testing Machine with a loading capacity of 1000kN. The failure modes and ultimate tensile loads were recorded for each sample.

Hereafter, all specimens are labelled for identification. The first letter indicates the type of steel, i.e. [H] for high strength steel and [M] for mild steel. The second letter indicates the

adhesive name: C = Sika Sikadur-330, N = Nippon adhesive and S = Spabond 345. The third letter indicates the CFRP type: W = Sika Wrap, S = Strand CFRP and P = CFRP pultruded plate. The specimens were given an extra number to indicate the number of CFRP layers on each side of the joint.

Table 7. MCW3 samples with different roughness values

Label	Roughness Ra (μm)	Ultimate tensile load (kN)	Failure mode
MCW3	0.73	60.5	Combination of cohesion failure and inter-laminar failure
MCW3	0.94	67.2	
MCW3	1.10	62.0	
MCW3	1.65	65.0	
MCW3	2.95	73.0	
MCW3	3.69	64.5	
MCW3	4.43	60.0	
MCW3	7.75	66.0	

The ultimate loading capacity versus roughness values are plotted in Figure 18. Clearly the variation of surface roughness in the range 0.73μm to 7.75μm did not change the ultimate load capacity. Due to the disadvantages of higher surface roughness, especially the difficulties associated with cleaning, lower surface roughness is recommended.

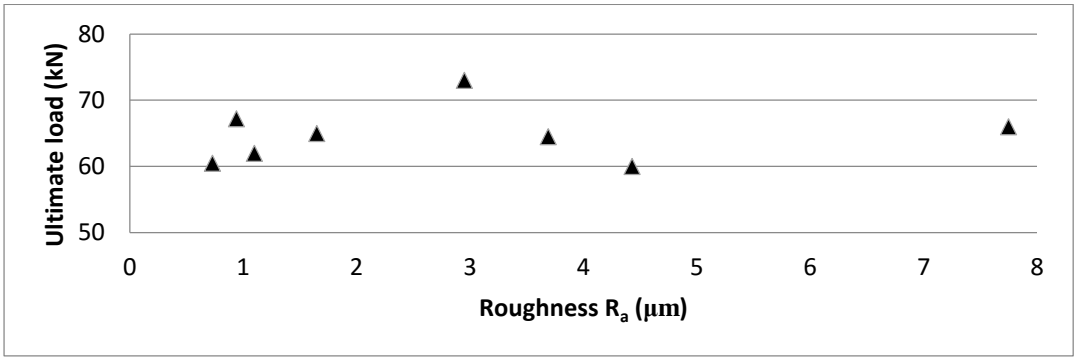

Figure 18. Tensile capacity versus surface roughness

4.6. Series 3: Influence of CFRP, adhesive type and steel stiffness on ultimate capacity

In this series, an additional 13 specimens were prepared with different adhesives, CFRP materials and steel types. The roughness values were also recorded for comparison. The test results are summarized in Table 8.

Table 8. Experimental parameters and results

	M (Mild steel)		H (High strength steel)		Failure mode
	Roughness R_a (μm)	Ultimate tensile load (kN)	Roughness R_a (μm)	Ultimate tensile load (kN)	
CP1	5.24 4.98 5.11 5.11	90.0 86.0 89.2 80.0	2.32 4.50	119 102	Cohesive failure
NS2	1.10 4.50	83.5 87.5	2.32 2.32 3.31	63.0 64.0 79.0	Adhesion failure at steel/adhesive interface
SW3	2.32 2.32	44.3 50.9			Inter-laminar failure of CFRP

The difference in roughness for high strength and mild steel was not compared in this study, due to the fact that no significant difference in roughness could be obtained on high strength steel using the methods adopted in this study. There is no obvious effect of steel strength on the tensile loading capacity of the joints. The high strength steel samples had a higher load capacity for the CP1 joint but a lower capacity for the NS2 joint. It is noted that there is a decrease in the ultimate load of HCP1 specimens with higher surface roughness. This difference in loads may be affected by the factors other than roughness. More tests and statistical hypothesis testing are needed to address this. It was found that there was a difference in the ultimate tensile load between MNS2 and HNS2 samples. These differences may be due to the fact that failure happened at the steel/adhesive interface. It appeared the high strength steel may not bond so well with the Nippon adhesive which reduced the ultimate loads of these samples.

A comparison between MNS2 and MCP1 showed that the bond strength was quite similar, though very slightly higher for MCP1 samples. The yield stress of the mild steel plate is normally 350MPa, so given the 5mm x 50mm cross-section the yield load is about 87.5kN. It

can be seen that the MCP1 specimens developed the full steel yield load, hence it is possible the joint strength could have exceeded this value. This is borne out by the higher HCP1 capacity. A cracking sound occurred before the specimens reached the steel yield load, indicating that the failure was ductile. This can also be considered as a "sign" that the structure will fail if the load is increased. It is hypothesised that when the steel yields the strain in the steel at the location close to the bonding area increases significantly. This increase leads to significant slip between CFRP ends and steel. Examination of the MCP1 samples after failure provided good evidence for this hypothesis. It was found that for the unfailed end of the sample, the excess adhesive that had hardened and stuck to the CFRP end had moved away from end, creating a gap due to the yielding of steel before failure as showed in Figure 19.

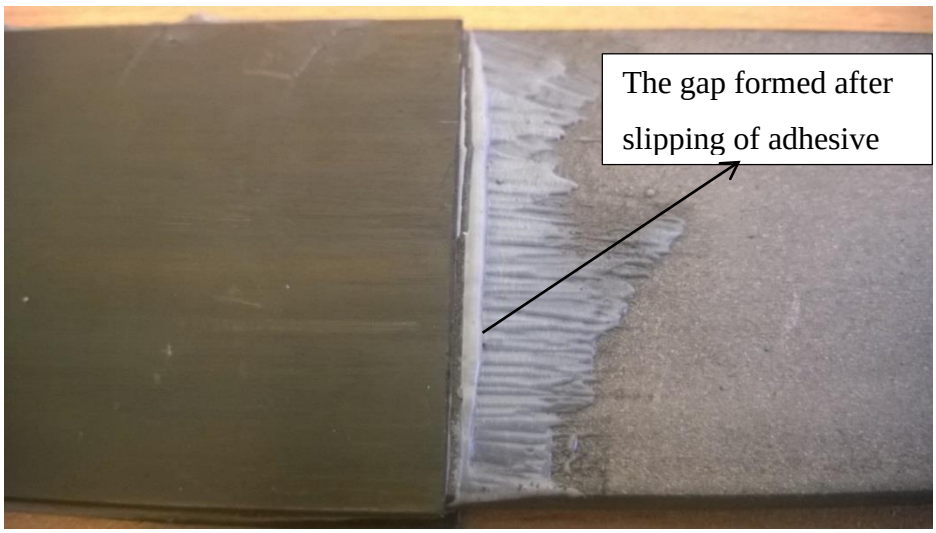

Figure 19. A significant slip occurred close to the CFRP end

As already noted, the HCP1 samples had higher ultimate loads than the MCP1 samples. The difference may be due to the properties of the steel. Since high strength steel did not yield at the failure loads, there was no significant increase in strain in the steel near the edge of the bonding area. It can be concluded that both HCP1 and MCP1 samples failed by adhesive properties (cohesive failure), but the main factor that affected the failure on HCP1 samples was the tensile load, and the failure of MCP1 samples was mainly due to the yielding of steel.

When the tensile load reached the steel yield load, a significant slip occurred close to CFRP ends that lead to initial failure, which rapidly transferred to the joint.

It can be seen that the occurrence of cohesive failure indicates that the optimal bonding has been achieved. This failure mode was found in common for all samples with a high loading capacity (MCP1 and HCP1 in Figure 20). Cohesive failure occurs within the adhesive layer and depends strongly on the adhesive properties. Therefore, flat surface CFRP plates are recommended for strengthening purposes since this failure mode is desirable. Cohesive failure was also obtained and recommended in (Fernando et al., 2013) by using grit blasting for surface treatment. However, by using CFRP plates, it can be concluded that sand or grit-blasting techniques are not necessary when strengthening steel structures with CFRP plates. Sand or grit-blasting are mainly applied in developed countries using a high pressure stream of abrasive material to remove the contaminant layer and produce a rough surface prior bonding. Grinding using abrasive discs is a common technique in many countries, the disc rotates at high speed generating high friction between the disc and the steel surface in order to remove the contaminant. The largest load capacity was found to be 73kN with the roughness of 2.95μm (Figure 18). This result matched the recommendation of using a 0.25mm grit blasting in (Fernando et al., 2013). The 0.25mm grit blasting produced an average total energy of 54.55mJ/m^2 with the corresponding roughness between 2 and 3μm.

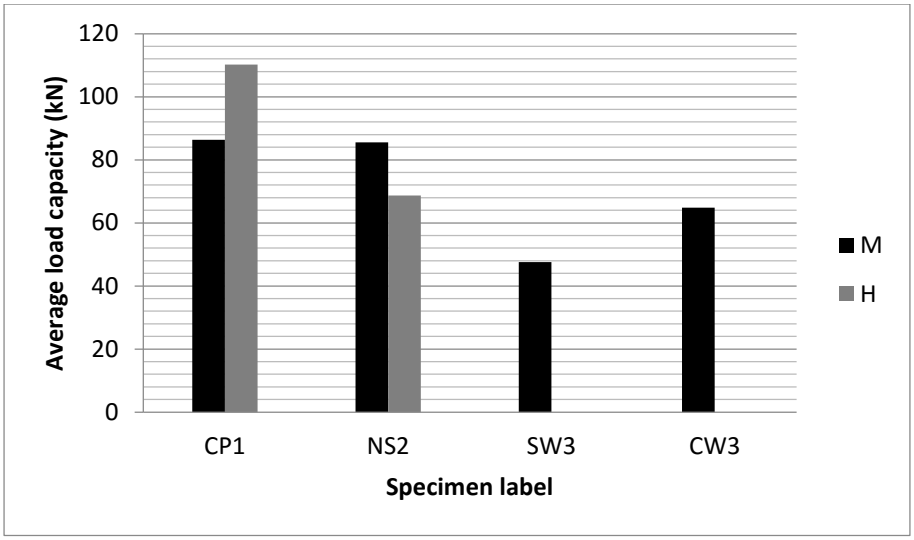

Figure 20. Ultimate load comparison of all specimens

All specimens labelled MSW3 failed by interlaminar failure within the CFRP due to a lack of adhesive penetrating inside CFRP fibres, which is undesirable (Figure 21b). Since the viscosity of Spabond 345 is much higher than Sikadur-330 (87Pa.s compared with 6Pa.s), Spabond 345 is more suitable with CFRP plates or strand sheets. Although Sikadur-330 adhesive could penetrate inside SikaWrap CFRP sheets, inter-laminar failure still occurred predominantly (Figure 21c) due to the internal bonding of the fibres being weaker than the external (surface) bonding. Therefore, low viscosity adhesives are more suitable when using CFRP woven sheets.

The specimens HNS2 failed by debonding. The failure occurred at the interface between the steel and primer resin. A similar failure mode was obtained by Jiao et al. (2014). Although the ultimate tensile loads are comparable with those obtained by other researchers (Liu et al., 2010), (Wu et al., 2012c) and (Bocciarelli et al., 2009), the failure occurred abruptly and is considered to be brittle failure. This may be due to the thickness of the primer resin. The manufacturer recommends an optimal amount of primer resin to be 150g/m^2, i.e. 0.125mm thick. In reality it is very difficult to control a uniform thin layer of epoxy resin. Jiao et al. (2014) showed that the primer resin did not reduce the ultimate loading capacity, but reduced the fatigue life of steel structures.

It can be concluded that the tensile load capacity of the double strap joint is affected significantly by the types of CFRP and the adhesive system. The MBrace Laminate is the most suitable for strengthening purposes. It can also be seen from Table 7 and Table 8 that the ultimate loads of all specimens strengthened with MBrace Laminate are similar although they were prepared with different roughness.

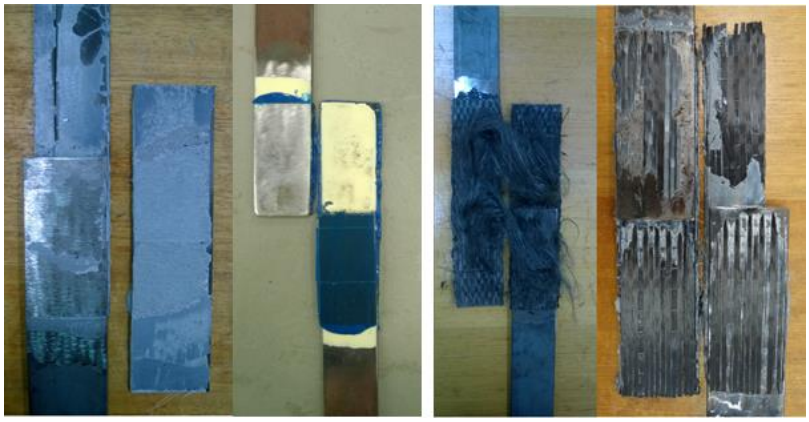

(a) (b) (c) (d)

Figure 21. Typical failure modes: (a) and (b) adhesion failure, (c) interlaminar failure, (d) inter-laminar and cohesive failure

The load versus strain charts were made by installing five strain gauges on one side of the CFRP on sample HCP1 and MCP1 (Figure 17a). Figure 22shows that failure initiated at the CFRP end for both mild and high strength steel specimens. A decrease in strain indicates cohesive failure at this location, which progressed gradually from the end towards the joint The strain then returned to zero due to the elastic behaviour of the CFRP. As expected significantly higher strain in the CFRP was found at the joint, since it is carrying the full load at that point because of the discontinuity in steel, and lower strain was found at the end of the CFRP where loads had not yet transferred from the steel into the CFRP. However, there was no significant variation in strain at mid locations. At failure, the largest strains of CFRP were about 0.36% and 0.57% for samples MCP1 and HCP1 respectively. This is because of the difference in ultimate load. It can be seen that at the failure point (90kN) for MCP1, the ultimate strain in the CFRP was found to be similar to that obtained for HCP1 (at 90kN).

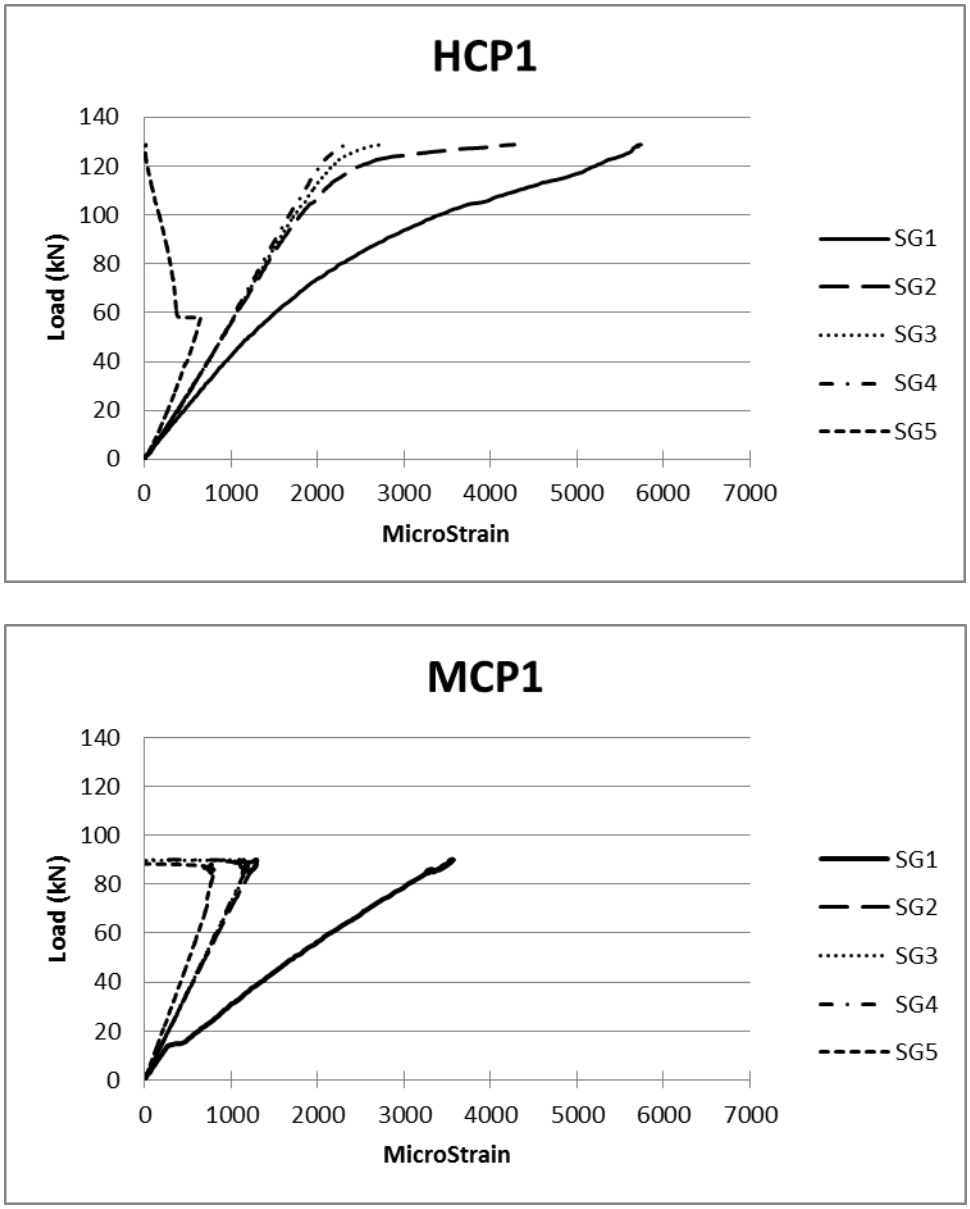

Figure 22. Load-strain curve of sample HCP1 (a) and MCP1 (b)

The charts demonstrate clearly the difference in behaviour between MCP1 and HCP1 samples. The strain in the HCP1 sample at the end CFRP (120mm from the joint) increased gradually with load until 60kN then decrease suddenly whereas in the MCP1 sample, the load versus strain is linear right up until failure. There was a significant increase in strain when the load was greater than 120kN at the location between 30 and 90mm from the joint. This increase in strain prior to failure indicated that ductile failure was obtained whereas the yield load of the high strength steel was about 220kN. That is, when the load reached 120kN, although the steel behaved linearly, the CFRP-adhesive-steel exhibited nonlinear or

hardening behaviour. In contrast, no hardening behaviour was found in sample MCP1 at the same locations (SG2-4), the strain was found to start decreasing when the load was close to the ultimate load. This indicates that the failure started to occur at the locations of SG4, SG3 and SG2 at almost the same time.

4.7. Conclusion and recommendation

The following conclusions are noted:

- The tensile capacity of double strap joints depends strongly on the types of CFRP. CFRP plates are recommended for flat surfaces since the application process is simpler and only one layer is required for bonding, hence human errors can be minimised. Strand CFRP sheets are also recommended for strengthening mild steel plate and can provide comparable results with the use of CFRP plates.
- The surface roughness in the range between 0.73μm and 7.75μm has no significant effect on either the bonding behaviour or the tensile capacity of the joints. Grinding may be suitable as an alternative to grit or sand blasting in the preparation process. The largest bond strength was found on the sample with the roughness of 2.95μm which was within the recommendation in (Fernando et al., 2013).
- A higher load capacity can be obtained using the combination of high strength steel and CFRP plates if the joint is not the limiting factor. Strand CFRP sheets are not recommended for high strength steel since the ultimate loads were much lower than for those specimens prepared with CFRP plates.
- The strain in the CFRP is highest at the joint and reduces significantly away from the joint. All samples showed linear behaviour when the loads were less than about 80kN. A hardening process was observed for high strength steel samples, whereas the behaviour was linear in the mild steel specimens.

- Cohesive failure was achieved by using grinding discs for those samples prepared with CFRP plates. Therefore the use of CFRP plates does not require sand or grit blasting techniques.

Chapter 5. FATIGUE BEHAVIOUR OF STRAND CFRP SHEETS CONNECTING STEEL PLATES

5.1. Introduction

Flexible CFRP sheets are often used to repair defected metallic structures that contain curved surfaces, such as circular hollow sections (Jiao and Zhao, 2004a, Teng et al., 2012a). The repair process generally involves an onsite wet layup process in which epoxy resin is evenly spread on the steel surface and between each CFRP layer. Unlike CFRP plates that are impregnated with resin under factory conditions, the quality of CFRP bonding through a wet layup process is affected by many factors, such as the types of CFRP and epoxy materials, ambient temperatures and the pot life of the epoxy resin. Air bubbles are often embedded between CFRP layers, causing the reduction in the bond strength of the composites. Researchers are using different method to increase the quality of the wet layup of CFRP, such as using vacuum bags (Jiao et al., 2012d). There have been other attempts in improving the manufacturing process of CFRP materials. Strand FRP sheet is a new type of CFRP material, in which CFRP fibre was impregnated with resin to form hardened strands at factory conditions, then the strands were tied together to form a sheet. Strand CFRP sheet are flexible and can be applied to the surface of a circular hollow section with the strands along the longitudinal direction of the tube. Recent tests on steel plates bonded with strand CFRP sheets showed promising results (Hidekuma et al. 2012). While static tests were conducted by some researchers on steel members strengthened with strand CFRP sheets, little research can be found on the fatigue behaviour of defected steel beams or double strap steel joints strengthened with CFRP strand sheets.

For steel structures subject to cyclic loading, both the bonding quality and the mechanical properties of CFRP materials are vital in increasing the fatigue strength of the repaired structures. Previous studies showed that high modulus CFRP materials were better performed in extending the fatigue life of cracked metallic structures (Liu et al. 2010; Jiao et al. 2012b).

Tabrizi et al. (2013) tested a steel beam strengthened with four layers of strand CFRP sheets. It was found that the strengthening system was effective to carry the fatigue load. In this study, two types of strand CFRP sheets manufactured by Nippon Steel Materials Co., Ltd in Japan were used to repair defected steel beams, and the high modulus strand sheets were used for the double strap steel joints. The Young's modulus of the strand sheets were 430GPa and 690GPa respectively. The test results were compared with previous data obtained from steel beams and double strap steel joints strengthened with conventional CFRP sheets and tested under the same testing configurations. The aim of this study is to examine the performance of strand CFRP sheets under cyclic loads.

5.2. Experimental details

5.2.1. Material properties

NIPPON Steel Materials Co., Ltd manufactured three types of strand sheets with low, medium and high Young's moduli. The tensile strengths of the medium and high moduli sheets used in this study are 4539MPa and 3010MPa respectively. These data were obtained from tensile tests conducted by the manufacturer in accordance with Japanese standard JIS A 1191 (JIS, 2004). The strands, with the diameter of about 1.2mm, were tied together by wires to form a CFRP strand sheet. The gap between each strand was about 0.5mm. Since CFRP strands were impregnated with resin, the unit weight of CFRP strand sheets is about 620g/m^2 which is higher than that of other CFRP sheets, such as MBrace CF530 that has a unit weight of around 400g/m^2. While the Young's modulus of high modulus strand sheets (FSS_HM600) is 690GPa, which is slightly higher than the nominal Young's modulus of 640GPa for MBrace CF530, the medium modulus strand sheet (FSS-MM600) has a Young's modulus of around 430GPa.

The epoxy resin used in this study was also manufactured by NIPPON Steel. Two types of resins were involved, the primer resin (FP-WE7W) and the bonding resin (FB-E9S). The

primer resin was a light yellow coloured two components epoxy that had a pot life of 34 minutes and a setting time of nine hours. It was required to be applied to the cleaned steel surface according to the manufacturer's instructions. When the primer resin was set at the room temperature after at least 12 hours, the bonding of strand sheets using the bonding resin, FB_E9S, can be started. The primer resin served to protect the steel surface from corrosion by preventing the direct contact of CFRP materials with the steel substrate. The effect of the primer resin on the bonding strength between CFRP and the steel was examined in this study. Based on the manufacturer's data sheet, the tensile strength of the bonding resin FB_E9S was 39MPa, whereas the tensile strength of the primer resin FP-WE7W was not specified. Since failure may happen in the interface between the primer resin and the steel substrate, the properties of the primer resin are vital for the fatigue strength of steel elements bonded with strand CFRP sheets. In order to obtain the properties of the primer and epoxy resin, tensile tests were conducted on FP-WE7W samples in accordance with Australian Standard AS3572.7 (SAA, 2002) that was for the testing of unreinforced resin. Three FB_E9S epoxy samples were also prepared and tested using the same testing method. Figure 23 shows the samples with the dimensions of 200 x 20 x 5 (length x width x thickness). Figure 24 shows the stress versus strain curves of the test samples. An average tensile strength of 30.7MPa and 20.6MPa was obtained for FB_E9S epoxy resin and the primer resin FP-WE7W respectively. It can be seen from Figure 24 that the FB_E9S epoxy resin is higher in tensile strength but lower in the ultimate strain comparing to those of the primer resin. It should be noted that the ultimate strain of the primer resin was not recorded by the applied strain gauge since it was larger than the measurement capacity of the strain gauge.

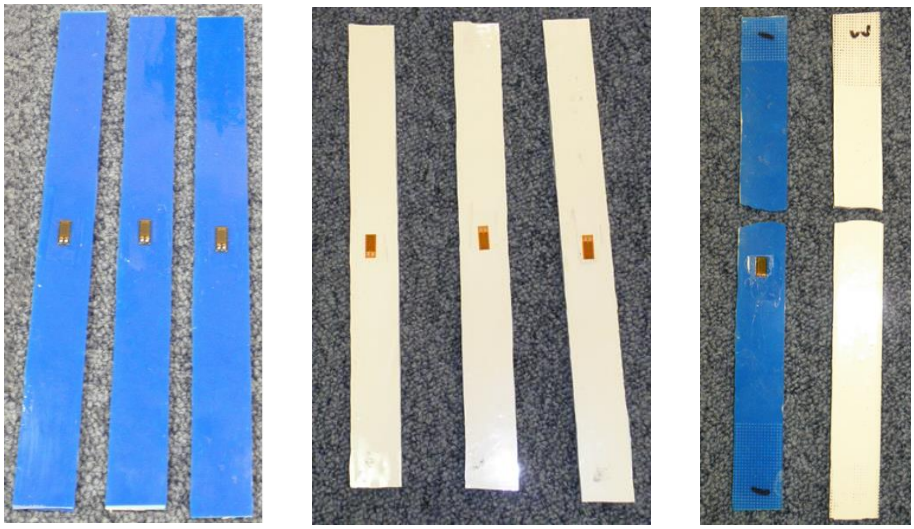

Figure 23. Epoxy tensile test samples

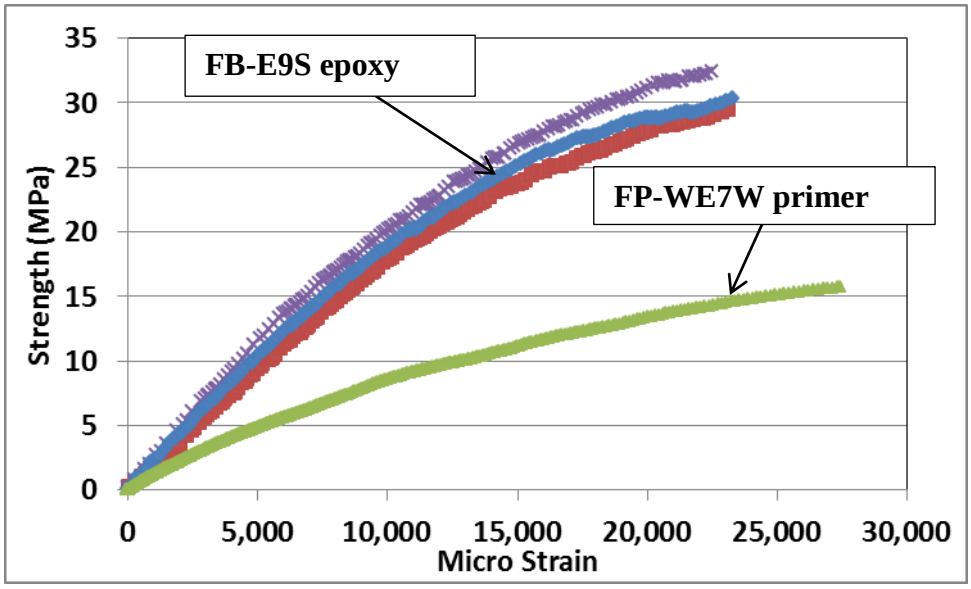

Figure 24. Stress and strain curves of the epoxy resins

The steel beams used in the tests were Grade 400 150UB14 that was manufactured by OneSteel Australia. The yield stress and ultimate tensile strength of the steel were 412MPa and 541MPa respectively with a Young's modulus of 207GPa (Jiao et al., 2012a). The yield stress and the ultimate tensile strength of the steel plate used for the double strap steel joints were 375MPa and 537MPa that were obtained through tensile coupon tests in accordance with AS1391 (SAA, 1991).

5.2.2. Specimen preparation

Fatigue tests of defected steel beams were conducted under four-point-bending. A total of eight beams were prepared. Each beam was 1.4m in length that was cut from a full length of 150UB14 section. The first step in the preparation was to make a cut in the mid-section of each beam. The purpose of the cut was to simulate a crack on the steel beam that may be caused by long term fatigue loading. The cut was 2mm in width and 22mm in depth measured from the tensile flange to part of the web. Then the defected beam was repaired by applying the strand CFRP sheet at the cut. It should be noted that the fatigue life of the strengthened beam was related to the size of the initial cut. The size of the cut was the same as those adopted in previous studies (Jiao et al., 2012a, Jiao et al., 2012c, Jiao et al., 2012d) in which CFRP sheets and plates were used. Therefore, the fatigue performance of the strand CFRP sheets in this study can be compared to those of CFRP materials. The cut was lightly welded on the beam sofit so that the epoxy resin could not flow into the cut during the repair. Then the weld was grinded flat and the area on both sides of the weld was cleaned using a grinder so that the rust was removed. The steel surface was cleaned with acetone for any grease and loose particles. In order to study the effect of the primer resin on bonding, two specimens were prepared with a layer of the primer resin and other specimens were prepared without the primer resin, i.e., strand sheets and FB-E9S epoxy were directly applied to the steel substrate. For specimens with the primer resin, the strand CFRP sheet was applied after the primer resin was applied and cured for 24 hours. The length of the strand CFRP sheet on both sides of the bonding was 100mm that was selected based on the effective bonded length of 75mm to 100mm for some CFRP and epoxy strengthened steel structures (Jiao & Zhao 2004; Fawzia et al. 2010). Figure 25 shows the details of the applied strand CFRP sheets in the region containing the notch. In order to examine the effect of the number of CFRP layers on the failure mode, four specimens were bonded with one layer of strand sheet and the other four specimens were bonded with two layers of strand sheets. When two layers of sheets were

applied, the layup of both layers were completed with one batch of epoxy, i.e., the second layer was applied before the resin in the first layer was hardened.

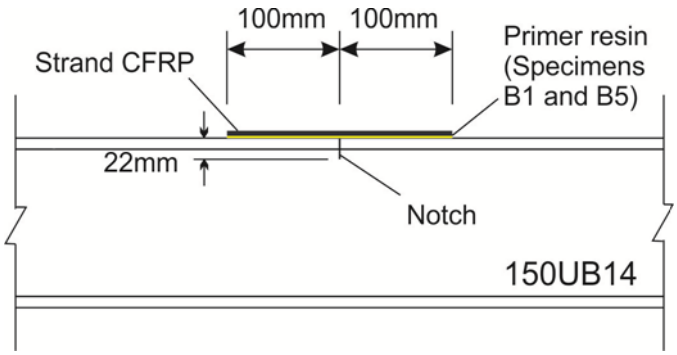

Figure 25. Details of strand CFRP sheets bonded to the notched beam

For the double strap steel specimens, four steps were taken in the preparation of each specimen that involved the primer resin. First of all, after the steel plates were cut to size and the surfaces cleaned in the same manner as for the steel beam specimens, the premier resin was evenly applied on one side of a specimen using a brush. Then after the premier resin was cured for 24 hours, the specimen was turned over and the primer resin was applied on the other side of the specimen. After another 24 hours when the primer resin was cued, two layers of CFRP sheets were applied with the FB-E9S resin on one side of the specimen. After it was cued for another 24 hours, the specimen was turned over again so that two layers of strand CFRP sheets were applied on the other side of the specimen. Therefore it would take at least four days to prepare a double strap specimen. Some double strap specimens were bonded without the primer resin. In this case, it took two days to apply the Strand sheets on both sides of the sample. Table 9 lists the details of all the specimens.

Table 9. List of specimens

Specimens	Label	Type of CFRP	No. of Strand CFRP layers	Applied with primer resin
Beams in four-point bending	B1	High modulus	1	Yes
	B2	High modulus	1	No
	B3	High modulus	2	No
	B4	High modulus	2	No
	B5	Medium modulus	1	Yes
	B6	Medium modulus	1	No
	B7	Medium modulus	2	No
	B8	Medium modulus	2	No
Double strap joints	T1	High modulus	4	No
	T2	High modulus	4	No
	T3	High modulus	4	No
	T4	High modulus	4	No
	T5	High modulus	4	Yes
	T6	High modulus	4	Yes
	T7	High modulus	4	Yes
	T8	High modulus	4	Yes

All specimens were cured for one week before testing. Figure 26 shows some specimens in preparation. From the specimen preparation process, it was found that the epoxy resins could easily fill the gaps between CFRP strands to form a composite. No vacuum bags were used in the layup process.

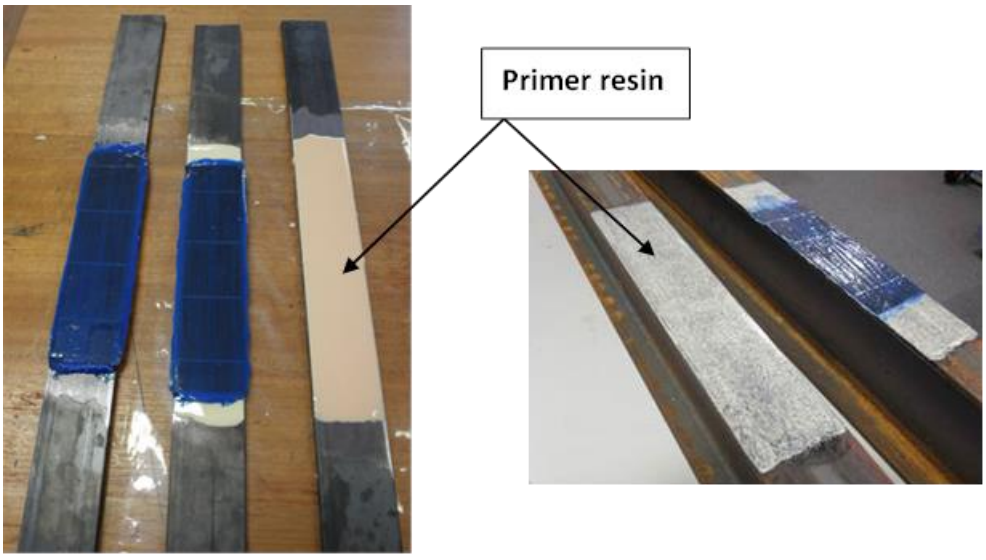

(a) (b)

Figure 26. Specimens in preparation (a) Double strap joints (b) steel beam

5.2.3. Test setup

Fatigue tests were conducted using a MTS machine with a loading capacity of 100kN. A four-point-bending rig was used to transfer the load from the MTS machine to a beam specimen with the details of the loading scheme shown in Figure 27.

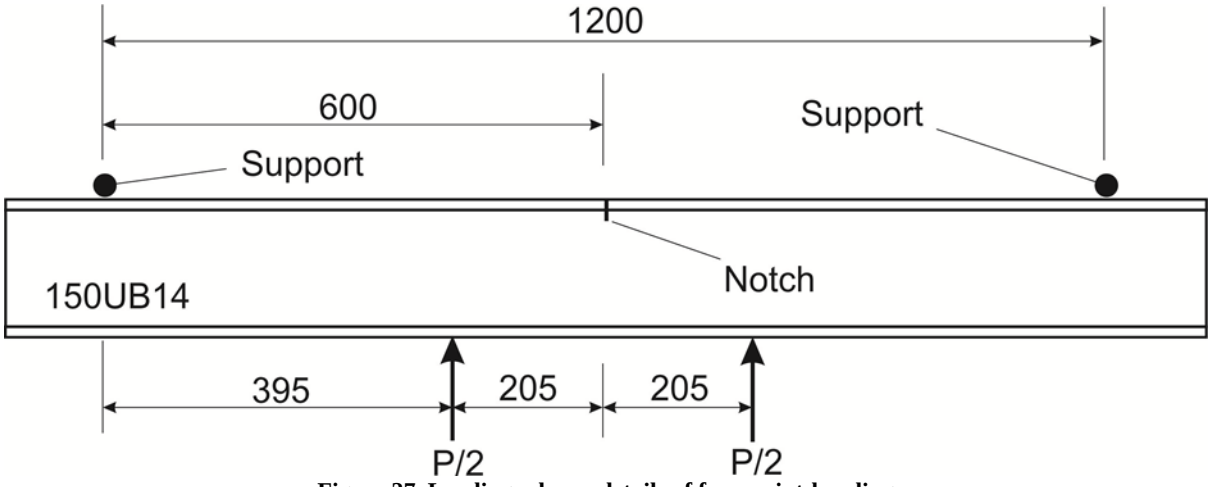

Figure 27. Loading scheme details of four-point-bending

The nominal stress range at the cut on the beam soffit of the gross section was calculated from Eqn 1 that was obtain from the aggregation of test data in (Jiao et al., 2012a). The minimum load to the maximum load ratio (i.e. stress ratio R) was 0.1.

$$\Delta\sigma = 2.336(1-R)P_{\max} \quad (1)$$

All specimens were tested to failure with a loading frequency of 5 Hz. The tests were conducted under the load control with a displacement trigger to stop the testing. A specimen was deemed failed when debonding or CFRP fibre breakage happened, causing excessive deflection and reaching the set displacement trigger so that the MTS machine stopped automatically. Figure 28 shows the test setup for the beams and double strap steel specimens.

Figure 28. Test setup (a) tension of double strap steel joints (b) steel beam in four-point bending

5.3. Test results

5.3.1. Failure modes

For beams under four point bending, all specimens failed by the debonding of CFRP sheets from the steel surface as shown in Figure 29(a), with the exception of specimen B2 that failed by the breakage of the strand sheet near the cut as shown in Figure 29(b). The fibre breakage failure indicated that more layers of CFRP sheets were required. The fibre breakage failure was avoided in the subsequent tests when two layers of strand sheets were applied.

(a) (b)

Figure 29. Failure modes of beams in bending (a) Debonding failure (Specimen B1) (b) Fibre breakage failure (Specimen B2)

For double strap steel joints, specimens failed by the debonding of the strand sheets in the interface between the steel and the epoxy resin for both specimens prepared with and without the primer resin. This failure mode was referred to as steel and adhesive interface failure by Zhao and Zhang (2007). Figure 30 shows some failed specimens. It should be noted that all the specimens in this study had a bond length of 100mm on either side of the crack for a beam specimen or measured from the centre of a double strap joint. By comparison with the experiments conducted by other researchers, fibre break failure happened for specimens when strand CFRP sheets were bonded over 3m length of the beams (Tabrizi et al., 2013).

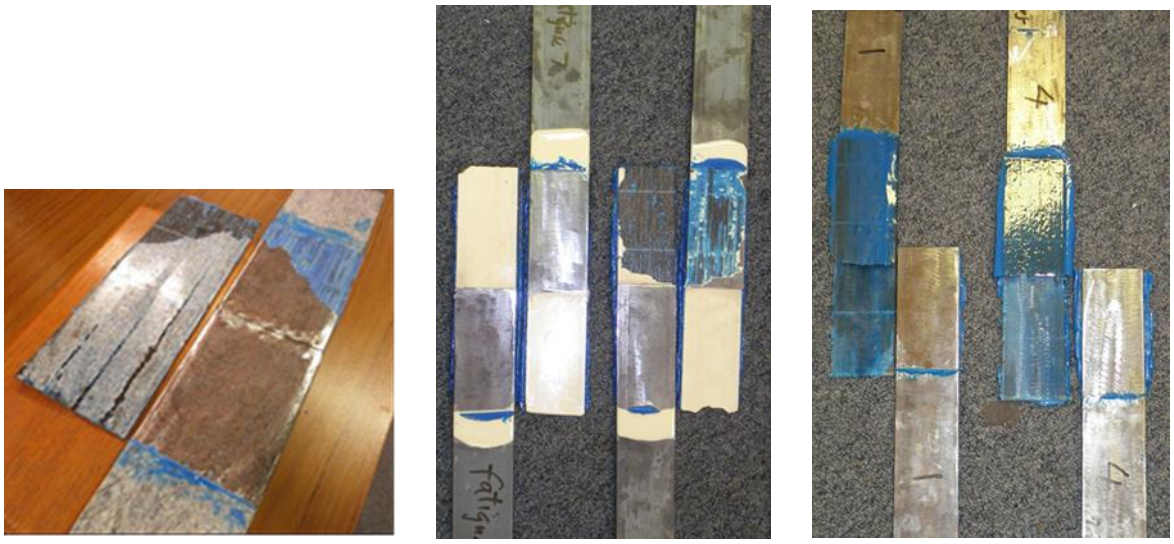

(a) (b) (c)

Figure 30. Debonding failure (a) Specimen B1 (b) Double strap joints with the primer resin (c) Double strap joints without the primer resin

5.3.2. Fatigue life

The number of cycles at failure and the stress range of all specimens are listed in Table 10. For the beams under four point bending, the stress range was calculated using Equation 1 based on the applied maximum load. The S-N data of all specimens are plotted in Figure 31 together with the data reported in (Jiao et al., 2012a, Jiao et al., 2012c) for beams strengthened with other CFRP sheets and CFRP plates that were tested under the same testing configuration.

Table 10. Fatigue life

Specimen	Label	Max Stress （MPa)	Min Stress （MPa)	Stress range (MPa)	Fatigue life	Failure mode
Beams in four-point bending	B1	70	7	63	290,912	Adhesion failure
	B2	70	7	63	348,367	CFRP breakage
	B3	70	7	63	511,703	Adhesive failure
	B4	77	8	69	310,064	Adhesive failure
	B5	70	7	63	154,757	Adhesion failure
	B6	70	7	63	405,580	Adhesive failure
	B7	63	6	57	486,403	Adhesive failure
	B8	77	8	69	371,052	Adhesive failure
Double strap joints	T1	80	8	72	1,243,500	Adhesive and steel
	T2	100	10	90	1,401,471	Adhesive and steel
	T3	120	12	108	360,647	Adhesive and steel
	T4	160	16	144	338,457	Adhesive and steel
	T5	120	12	108	80,243	Adhesive and steel
	T6	120	12	108	78,221	Adhesive and steel
	T7	120	12	108	85,681	Adhesive and steel
	T8	160	16	144	101, 21	Adhesive and steel

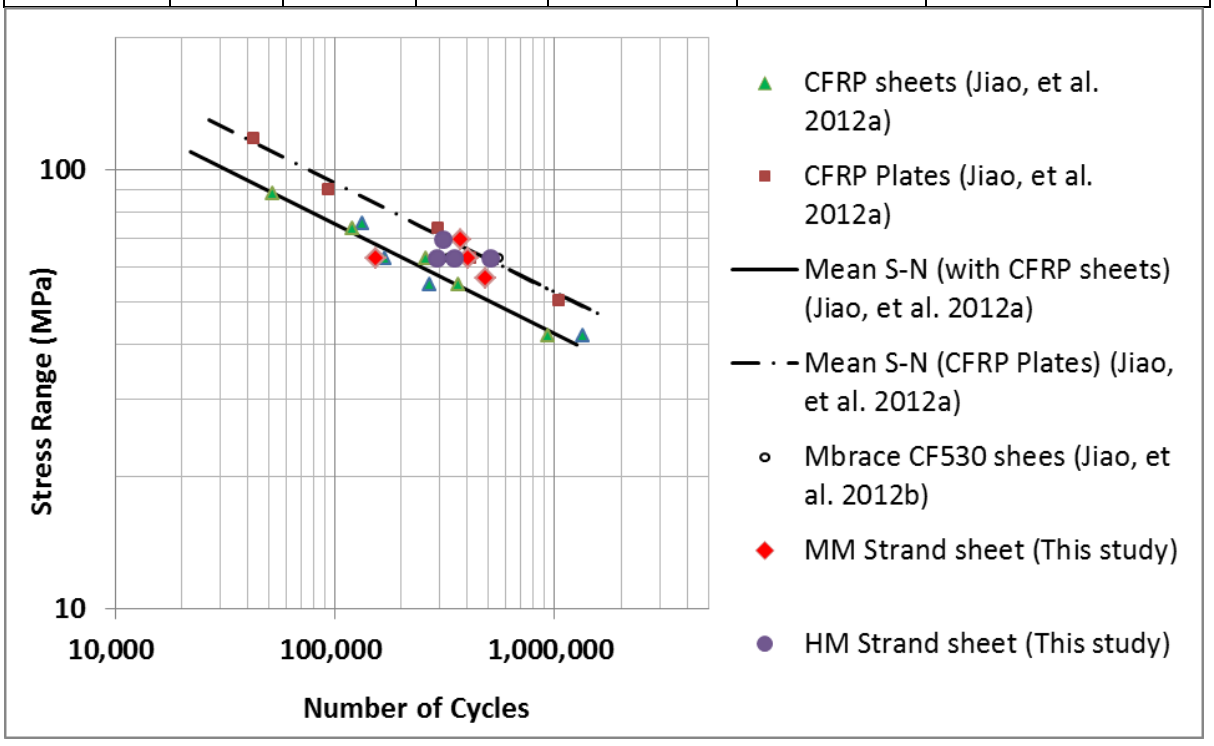

Figure 31. S-N plot of beams subject to four-point bending

It can be seen from Table 10 that the fatigue life of the two beams prepared with the primer resin is lower than those strengthened without the primer resin. This may be due to the lower

Young's modulus of the primer resin or thick adhesive layer (Liu et al. 2009). The test results showed that the fatigue life of the beams strengthened with the strand CFRP sheets without the primer resin were comparable to those beams strengthened with Sika CarboDur M1214 pultruded plates and those strengthened with high modulus MBrace CF530 sheets (Jiao et al., 2012c). In addition, no substantial difference in fatigue life was found between the medium and high modulus CFRP strand sheets.

For the double strap steel joints under axial tension, the fatigue cycles at failure of the eight specimens bonded with and without the primer resin are listed in Table 11 and plotted in Figure 32 together with the data reported by other researchers. It can be seen from Figure 32 that the double strap steel joints bonded with the FB-E9S resin and high modulus strand sheets are similar to those steel/CFRP joints bonded with MBrace CFRP sheets or laminates and Araldite 420 (Liu et al., 2005, Wu et al., 2012b) and Sika Cabodur CFRP sheets and Sikadur 30 epoxy (Bocciarelli et al., 2009, Colombi and Fava, 2012), whereas the fatigue life of the specimens bonded with the primer resin are lower than that of the specimens without the primer resin.

Table 11. Comparison of fatigue life

Specimens (1)	Fatigue life		Stress range (MPa) (4)	log_10(Stress range)	Fatigue life ratio of (2) / (3)
	Bonded with primer resin (2)	Bonded without primer resin (3)			
Beams in four-point	290, 912	511, 703	63	1.80	0.57
	154, 757	405, 580	63	1.80	0.38
Double strap joints	80, 243	360, 647	108	2.03	0.22
	78, 221	360, 647	108	2.03	0.22
	85, 681	360, 647	108	2.03	0.24
	101, 021	338, 457	144	2.16	0.30

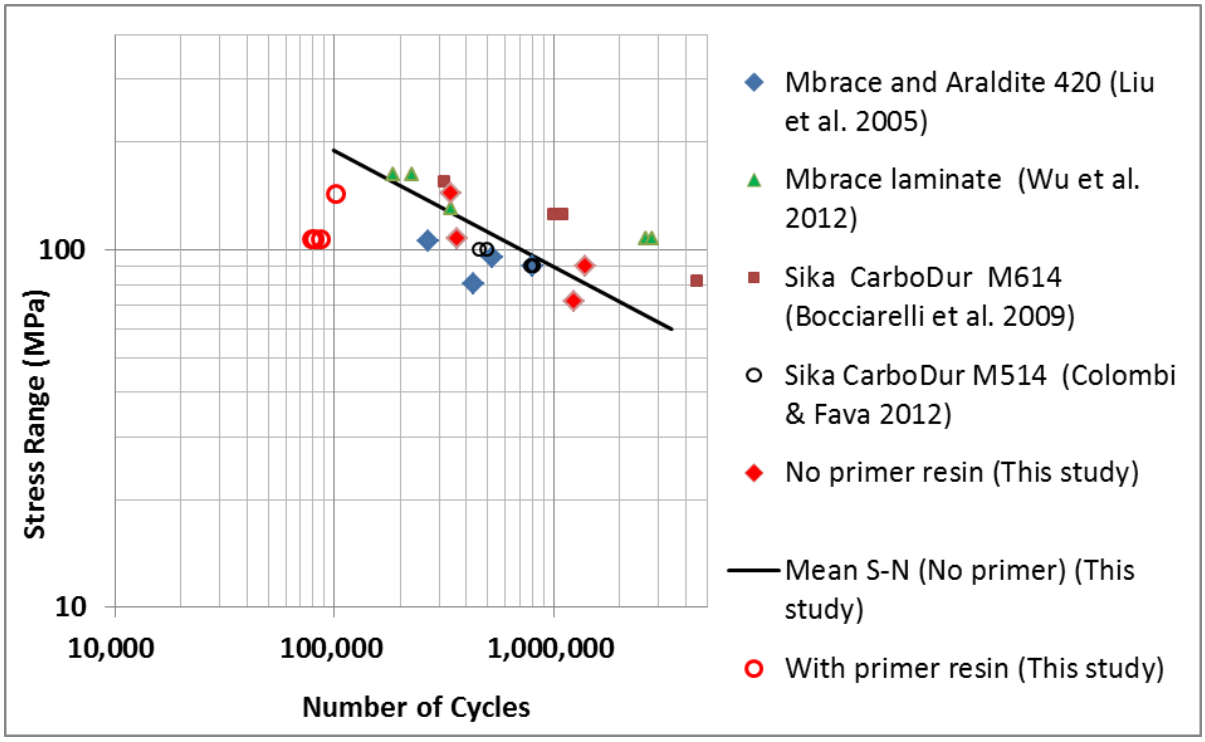

Figure 32. S-N plot of double strap steel joints subject to axial tensile fatigue load

Table 11 shows a comparison of the fatigue life of specimens bonded with and without the primer resin. A reduction factor in fatigue life was defined as the ratio of the fatigue life of specimens bonded with and without the primer resin under the same loading condition. The reduction factors are plotted in Figure 33 against the stress range in log10 scale. It can be seen that there is a linear reduction in fatigue life with the increase of the stress range when the premier resin was used.

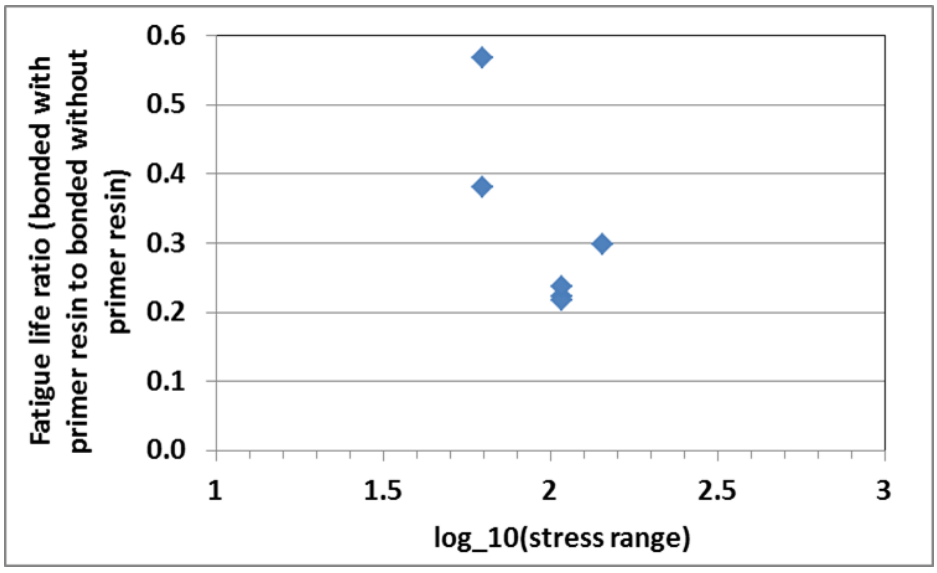

Figure 33. Fatigue life reduction factors versus stress range in log10 scale

5.4. Conclusion

This study investigated the fatigue behaviour of steel beams and double strap steel joints bonded with high and medium moduli strand CFRP sheets. Based on the limited test results, the following conclusions were obtained:

- The fatigue life of beams strengthened with high or medium CFRP strand sheets was comparable to that of beams strengthened with MBrace CF530 high modulus CFRP sheets and Sika Cabodur M1214 CFRP plates regarding to the fatigue life and the loading stress. However, the use of CFRP strand sheets showed more advantages against the conventional CFRP materials during the preparation process since no vacuum bags were needed.
- The primer resin caused a linear reduction in fatigue life with the increase of the stress range. This may be due to the lower Young's modulus of the primer resin or the thick adhesive layer, causing adhesion failure in the interface between the steel and the primer resin.
- At least two layers of strand CFRP sheets should be applied to the defected beams subject to cyclic loading in order to take the advantage of high strength of CFRP and to avoid the fibre breakage failure.
- The high and medium moduli CFRP strand sheets showed similar performance in extending the fatigue life of defected steel beams.

Chapter 6. A FINITE ELEMENT MODEL FOR PREDICTING ULTIMATE TENSILE CAPACITY OF DOUBLE-LAP ADHESIVE JOINTS

6.1. Introduction

The use of carbon fibre reinforced polymer (CFRP) for repairing and rehabilitating steel structures has increased rapidly in recent years. CFRP was first used to rehabilitate and strengthen the Delaware Bridge 1-704 in the United States (Mertz et al., 2002), and the Hythe and Slattocks Bridges in the UK (Luke and Consulting, 2001). These pioneering projects show the capability of CFRP to increase the load capacity without using traditional methods such as welding and bolting. Furthermore the application of CFRP is a very simple process due to its high strength – light weight, lower labour demands and rapid installation time.

The common failure mode of structures with composite laminates is delamination, particularly for CFRP-to-steel structures. This failure occurs due to the low resistance at the interface and depends strongly on the bond-slip relationship between adherents. In other words, the properties of the adhesive play a critical role in the bond strength. For double strap joints the interface bonding of both steel to adhesive and CFRP to adhesive affects the load capacity and delamination is likely to occur within the adhesive layer. Some researchers have established bond-slip models from experimental results. Xia and Teng (2005) and proposed simple bi-linear bond-slip models with the relationship between the slip at debonding δ_f and at peak shear stress δ_1 as shown in Figure 34. However, the effects of adhesive thickness and its nonlinear properties were not included in either of these or similar bi-linear models. A new tri-linear bond-slip model was established by Dehghani et al. (2012) and showed that the adhesive thickness did not affect the bonding capacity of the specimens (Figure 35).

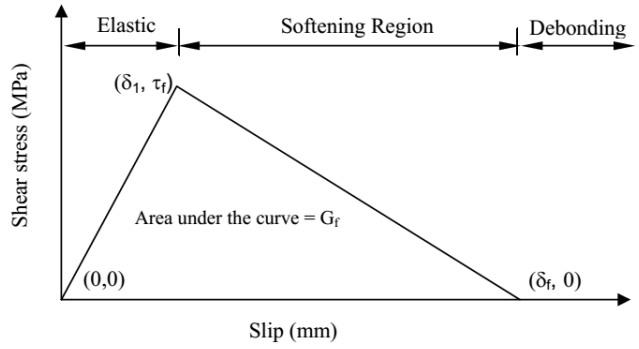

Figure 34. Bilinear bond-slip model (Xia and Teng, 2005)

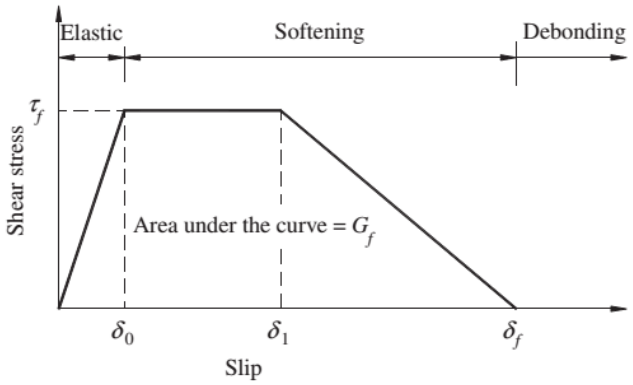

Figure 35. Trilinear bond-slip model (Dehghani et al., 2012)

It was found that by adding a plastic part ($\delta_0 \rightarrow \delta_1$ in Figure 35) the ultimate load could be predicted more accurately by the tri-linear model, showing good agreement with experiment in the case of CFRP-steel samples (Dehghani et al., 2012). However, these experiments were set up for pure shear force only. Double strap joints might behave slightly differently due to the presence of a small bending moment in the CFRP layers, reaching a maximum where they bridge the gap between the two steel members being joined. When comparing two adhesives, Yu et al. (2012) found that adhesives with a high elastic modulus, such as Sika Sikadur 330, might cause a more localised increase in the bending moment at the load end of the CFRP. Furthermore, few finite element models have been used to predict the ultimate load capacity of double strap joint samples.

The focus of this study is to develop a 2-D finite element model to study the effects of the adhesive's properties on the bond strength of double-strap joints. Since the objectives of this study were to predict the ultimate strength and the effective bond length, a 2-D model was capable to perform the tasks. Furthermore, a 2-D model required less computer resources than 3-D model so that it is more effective to perform the 2-D model. The ultimate loads predicted by the model were compared with the experimental results reported by Phan et al. (2015). The CFRP bond length and the steel strength were considered as the parameters in the model.

6.2. Finite element model and theoretical analysis

A lap joint may be described by relatively simple differential equations to predict the ultimate load. However, in the presence of failure such as yielding or peeling of the materials, these equations become very complicated for analysis (da Silva and Campilho, 2012). The finite element method (FEM) is one of the major numerical methods for solving these equations, especially when analysing adhesive joints. In this study, a two-dimensional nonlinear finite element analysis was performed by using ABAQUS. The FEM in ABAQUS was integrated with predefined options for analysis with adhesive bonding such as temperature, field variables, equivalent pressure stress, cohesive zone or mass flow rate. The initial failure criteria are defined such as crack growth or composite delamination.

Debonding of CFRP was analysed using the cohesive zone method (CZM) using the so-called cohesive damage models. The interface between the two separated adherents (i.e. the adhesive layer) was modelled with cohesive elements. This layer was chosen because failure was known to occur here, thus it is the weak link (Phan et al., 2015). These CZM elements could be created based on the traction-separation law with zero thickness or finite thickness. The zero-thickness element was chosen in this study due to several reasons: firstly, it has

been shown that the final results are unaffected by whether a finite or zero thickness CZM is used (Julian and Jofre, 2013) (Barbero, 2013); secondly, it was reported by Xia and Teng (2005) that when the adhesive thickness was less than 2mm, it did not affect the bond behaviour in experiments; and finally, elements with zero thickness could be useful in the case of laminated composites (Barbero, 2013) as they greatly facilitate building up of the model. Therefore, the adhesive thickness was not considered as a significant variable in the FEM and a constant thickness of 1mm was assigned. The basic concept of zero-thickness elements is that the layer is initially set up with a finite thickness (that is 1mm) in order to allow manipulating and defining of constraints. This could be done by adding an overlay element representing the adhesive layer as shown in Figure 36 (between the red lines). A master-slave technique was adopted to constrain the top adhesive surface (Slave 1) to the bottom layer of the CFRP (Master 1) and constrain the bottom adhesive surface (Slave 2) to top layer of the steel (Master 2). It should be noticed that the Master 1 and 2 are different and there is no direct contact between them. During the analysis, the Slave and Master could become separated causing debonding to occur.

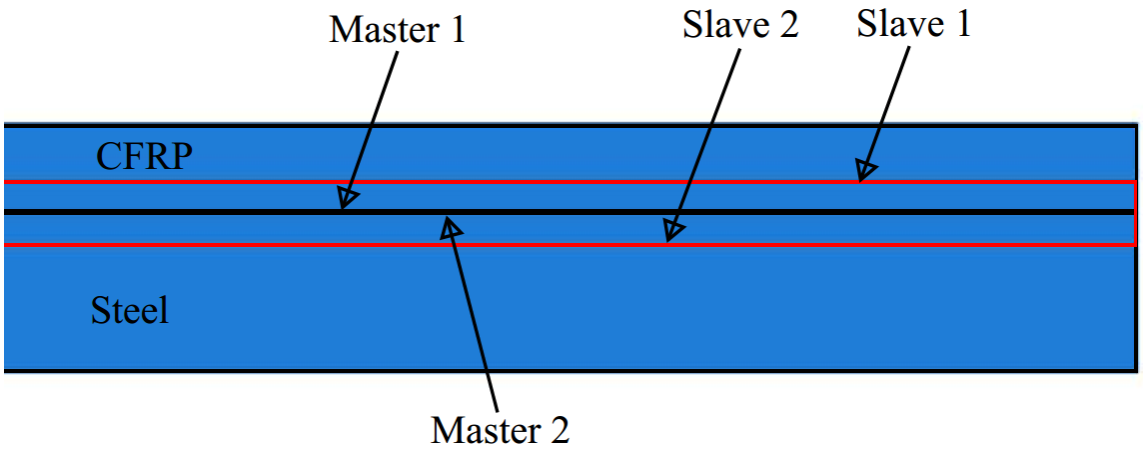

Figure 36. Master-Slave constraint for zero thickness adhesive, the red rectangular represents adhesive element

When using the CZM the engineering stress-strain relationship (σ and ϵ) was replaced by a traction-separation relationship (σ and δ) as shown in Figure 37. The slope of line OA was

defined as the penalty stiffness K – the stiffness of the material interface (Barbero, 2013). In this study, $K=K_{coh}$ since the adhesive was the the cohesive elements. Therefore, the traction separation can be described as

$$\sigma = (1 - D)K_{coh}\delta \qquad (1)$$

where δ is the corresponding separation between the CFRP and steel, σ is the surface traction and D is the damage parameter, initially zero while $\delta \leq \delta_0$.

The line AC in Figure 37 represents the linear softening of the joint, beginning with zero damage parameter $D=0$ at $\delta \leq \delta_0$ and ending with $D=1$ when $\delta \geq \delta_c$ (point C). $0 < D < 1$ when the specimen is losing its stiffness gradually, while D=0 on line OA, thus

$$D = \begin{cases} 0 & if\ \delta \leq \delta_0 \\ \dfrac{(\delta - \delta_0)\delta_c}{(\delta_c - \delta_0)\delta} & if\ \delta_0 < \delta < \delta_c \\ 1 & if\ \delta \geq \delta_c \end{cases} \qquad (2)$$

σ_{max} and δ_c are the output variables representing the ultimate tensile load and the critical effective vertical separation, respectively. The numerical model's results are expected to be similar to the graph in Figure 37 except the separation axis is replaced by the horizontal displacement between CFRP and steel. Point A the ultimate load corresponding to the effective bond length. Point B is a partially loaded/unloaded point and path BO represents a cohesive zone element being unloaded while partially damaged. In this case the stiffness is reduced. If the load is resumed after reducing stiffness, the stress path will follow triangle OBC.

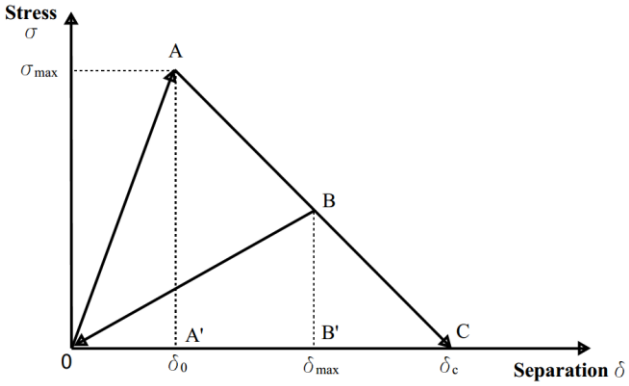

Figure 37. CZM stress transfer

6.2.1. Geometry and boundary conditions

The geometry and boundary conditions of the 2D plane stress finite element model are shown in Figure 38. Due to the double symmetry only one quarter of the joint was modelled as shown in Figure 38(b) in order to save time for the analysis.

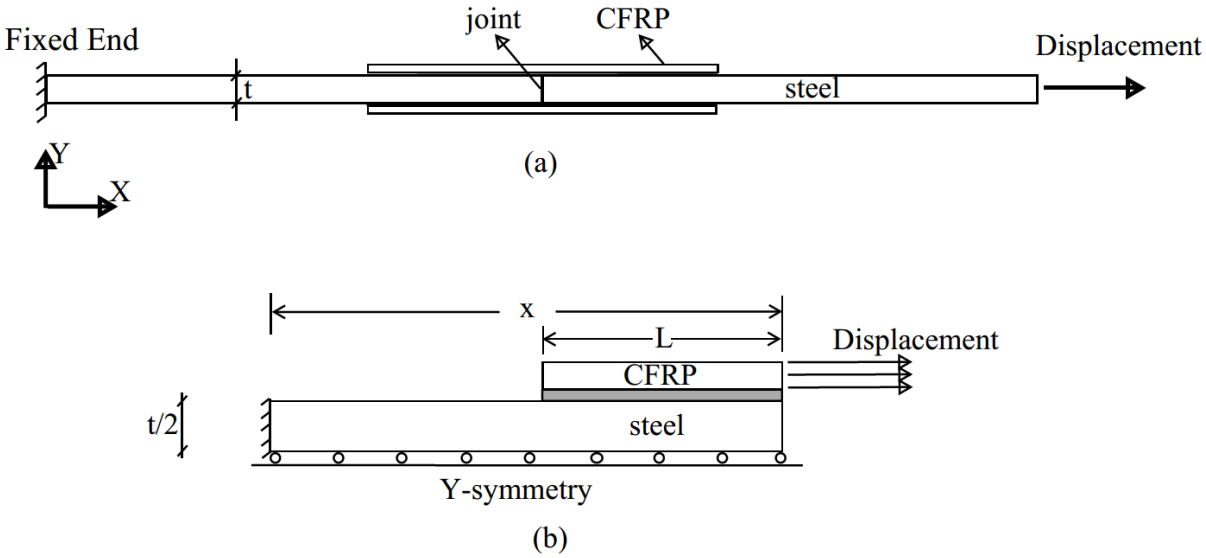

Figure 38. Boundary conditions of the specimen (Not to scale) (a) full model and (b) one quarter of the sample and its boundary conditions

The geometrical parameters are: $\frac{t}{2} = 2.5mm, x = 300mm$ and the bond length L is varied from 90mm to 170mm.

The steel plate was set to be fixed at the left end and free at the joint. A symmetric boundary condition (y-displacement and rotation about x and z axis were set to 0) was set at the bottom face of the steel as shown in Figure 38(b). In order to obtain accurate results, the geometrical non-linearity for large displacement was turned on. The displacement was assigned only in the X-direction and the reaction forces were recorded at the fixed (left) end of the steel.

6.2.2. Related material properties used in ABAQUS

In this study, both mild and high strength steels were investigated since some difference may be expected in the effective bond length due to the different stress-strain relationships of mild and high strength steels. The properties of steel were obtained by tensile coupon tests in accordance with AS1391 (SAA1991).

Properties of adhesive Sika Sikadur-330 and MBrace laminate CFRP were taken from the manufacturer's specifications. Table 12 shows the properties of these materials.

Table 12. Material properties

	Mild steel	High strength steel	CFRP	Adhesive
Elastic modulus (GPa)	187	206	170	4.5
Yield stress (MPa)	350	1100	-	-
Tensile strength (MPa)	541	1362	3100	30
Ultimate strain (%)	5.18	1.37	1.6	0.9

True stress and true strain were used to define the plasticity data in ABAQUS. Since the material test data were supplied as nominal stress and strain the formulas to convert between true strain/stress and nominal strain/stress are

$$\varepsilon = \ln(1 + \varepsilon_{nom}) \qquad (3)$$

$$\sigma = \sigma_{nom}(1 + \varepsilon_{nom}) \qquad (4)$$

Where ε and σ are the true strain and stress and ε_{nom} and σ_{nom} are the nominal strain and stress, respectively. It should be noted that equations (3) and (4) are only valid prior to the necking of the material.

Table 13 shows the stress/strain values of the mild and high strength steel that were input in ABAQUS non-linear material model.

Table 13. Stress-strain data for steel

Mild steel		**High strength steel**	
Strain	Stress (MPa)	Strain	Stress (MPa)
0.0000	0	0.000000	0
0.0018	360	0.004139	826
0.0240	400	0.004823	934
0.0303	433	0.005950	1073
0.0400	470	0.007820	1190
0.0500	550	0.010000	1256
		0.013892	1312

The steel had a Poisson's ratio of 0.3 and was modelled using solid homogeneous continuum elements. The stress-strain data in

Table 13 were defined using the material calibration capability. This process determined the elastic and plastic behaviour of the steel from the test data.

Solid homogeneous two-dimensional CFRP continuum elements with the thickness of 1.4mm, elastic modulus E=170GPa, Poisson's ratio of 0.3 and tensile strength of 3100MPa were input in ABAQUS.

Since the failure was predicted to occur at the adhesive layer, the adhesive properties were the critical parameters. The adhesive properties were input with the damage evolution which was defined in ABAQUS to specify the material damage initiation criteria. This step defined how the bonding degraded after the initiation criteria occurred. Another important parameter that was input in ABAQUS was the damage tolerance. The damage tolerance was defined as the flaws required in the sample to cause complete failure. In this study, failure was expected to occur at the adhesive layer over the bond length of the sample so that the tolerance was set to be equal to the bond length. The following parameters were input in ABAQUS:

- Shear strength = 12MPa (Damage initiation – QUADS damage)
- The fracture energy was estimated using the following equation (Xia and Teng, 2005)

$$G_f = 0.5\tau_f\delta_f$$

$$G_f = 0.5 \times 12 \times 0.4 = 2400\ \mathrm{J/m^2}$$

Where G_f is the fracture energy, τ_f is the shear stress and δ_f is the displacement at failure.

6.2.3. Meshing

The steel plate and the CFRP were modelled with 4-node bilinear plane stress quadrilateral incompatible modes elements (CPS4I). CPS4I stands for plane stress elements with 4-node bilinear, incompatible modes which is suitable for contact problem (ABAQUS, 2013). The incompatible modes aimed to improve the bending behaviour of the pure displacement elements. Since the mesh sensitive analysis was not available in ABAQUS, the mesh refinement study was conducted by tabulating the results then the final mesh size was chosen for the model. The "structured" meshing technique was used with a mesh size of 0.5mm for steel plate and CFRP. The adhesive layer was meshed with a "sweep" technique and 4-node cohesive elements (COH2D4) with a mesh size of 0.5mm. COH2D4 represents a 4-node two-dimensional cohesive element. The structured meshing technique could be applied for simple 2-D regions while the swept meshing technique was suitable for more complicated regions,

especially for the initial damaged region (ABAQUS, 2013). It was noted that the adhesive layer must be tested in order to determine if it was meshable using the swept meshing technique. Figure 39 shows the mesh details for all parts.

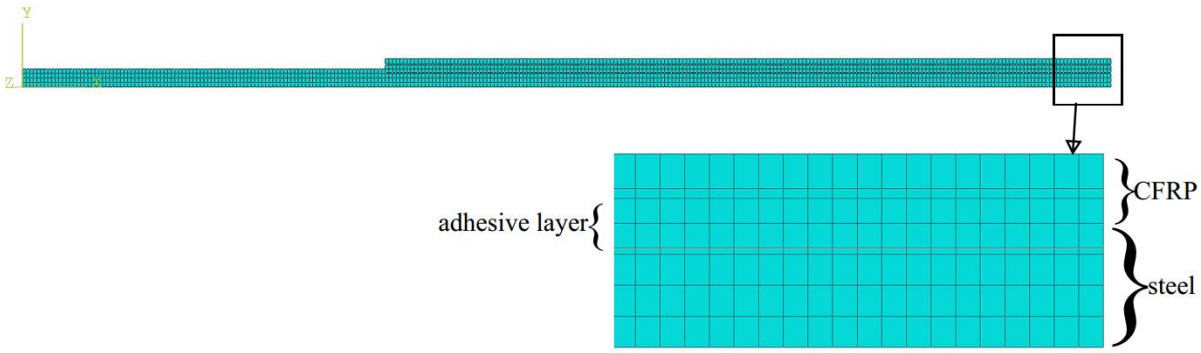

Figure 39. Mesh details

6.3. Results and discussion

6.3.1. Effective bond length

The finite element model was displacement controlled with the reaction force at the fixed end of the steel being recorded. This reaction force was only a half of the ultimate load of the full sample. Therefore, the recorded load must be multiplied by 2 prior to plotting. The load versus displacement for various lap lengths (L in Figure 38(b)) is plotted in Figure 40 and Figure 41 for the high strength and mild steel samples respectively.

For the high strength steel specimens, it can be seen from Figure 40 that the effective bond length was about 150mm, since the maximum load did not increase with further increase of the bond length. The ultimate load increased approximately linearly (from 71.9kN to 135.8kN) when the bond length was increased from 75mm to 150mm. However, further increase in the bond length to 200mm did not improve the ultimate load but increased the slip between the CFRP and steel. Figure 40 shows abrupt failure for samples with a bond length less than 150mm, but when the bond length was greater than 150mm the load started to plateau before failure, indicating an increase in the displacement prior to failure. This

suggested that although increasing the bond length further than the effective bond length did not enhance the ultimate load, it improved the ductility of the sample.

With the same configurations, Phan et al. (2015) found that the effective bond length was about 100mm which was different from the results obtained by the FE model. This is discussed in detail below and may be due to the increasing imperfection in the bond quality when bond length is increased. More tests are required in the future to verify this.

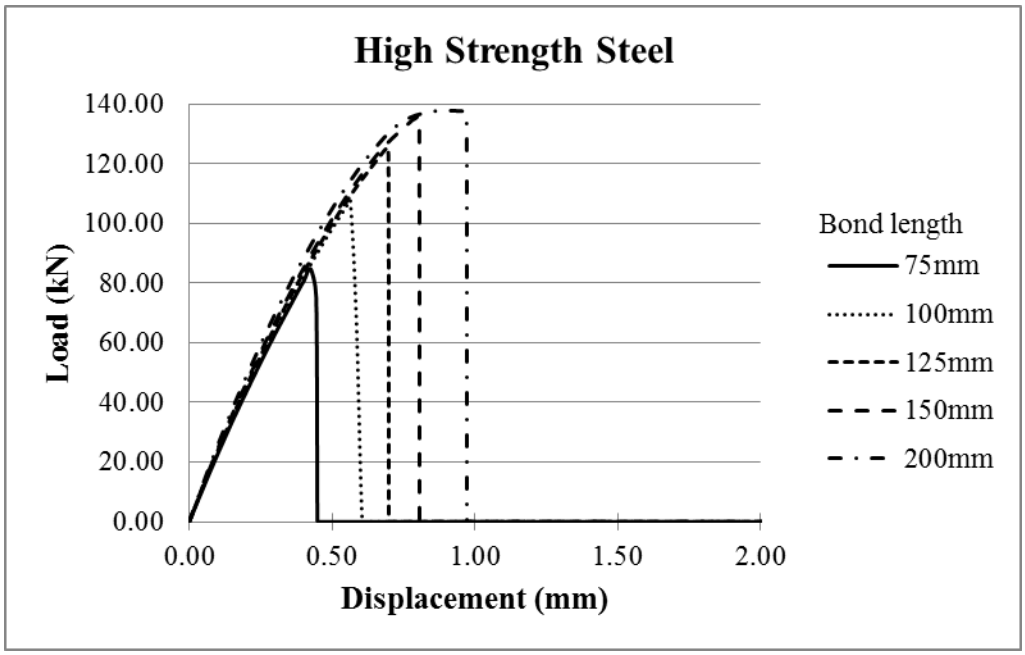

Figure 40. Load versus displacement for various bond lengths on high strength steel

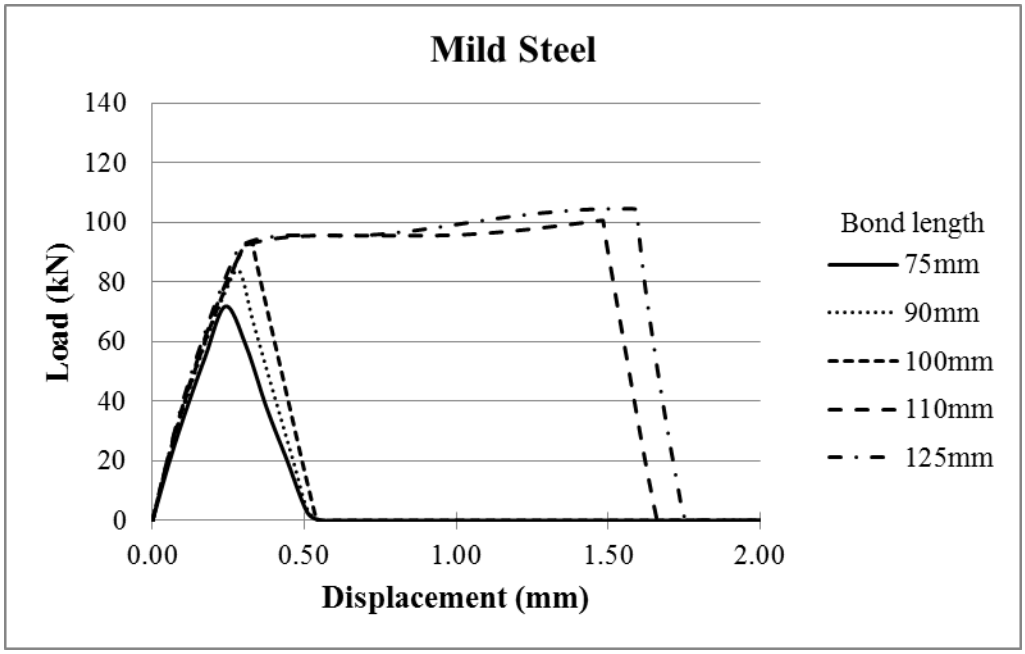

Figure 41. Load versus displacement for various bond lengths on mild steel

For mild steel samples, the effective bond length was found to be about 100mm, as shown in Figure 41. The CFRP strengthened mild steel samples failed mainly by steel yielding. The yield load of the steel plate in this study was about 90kN. Further increase in the bond length caused more yielding of the steel plate indicating that the yield stress of the steel plate limited the bond strength of the joint. The steel grade might also lead to the reduction in the effective bond length. A comparison between simulations of the mild and high strength steel samples shows different behaviour after reaching the ultimate load. In contrast to the high strength steel samples, a gradual reduction in load occurred after the ultimate load was reached in the mild steel samples, suggesting that the failure was ductile. Furthermore, when the bond length was less than 100mm, ultimate failure occurred with the same displacement of about 0.51mm. It must also be noted that with a given bond length, a higher load was obtained for the sample with high strength steel.

It can be seen that for those samples with the bond length greater than the effective bond length, there is a similarity between the load-displacement model and the bond-slip model

suggested by Dehghani et al. (2012) (Figure 37). It was noted that the bond-slip model could be achieved by a bond length which is greater than the effective bond length. This agreement confirms that the tri-linear model is more suitable for analysis rather than bi-linear model.

From the observations above it appears that the load carrying capacity and the effective bond length of CFRP strengthened double strap joints were limited by the steel grade. Once the steel yield stress was reached, failure occurred irrespective of a higher bonding property of the epoxy resin. Although the load carrying capacity was found to be greater for samples with high strength steel plates, the failure was brittle except for samples where the bond length was greater than the effective bond length. This is in spite of significant ductility in the mild steel material model. Ductility was observed on all samples with mild steel plates.

6.3.2. Result comparison

As mentioned earlier, the effective bond length was found to be 150mm and 100mm for high strength and mild steel samples, respectively. The mild steel results agreed with experiments reported by Phan et al. (2015) as shown in Table 14. However for the high strength steel samples, although the ultimate load agreed well at a bond lengths of 75mm and 125mm, the inferred effective bond length differed significantly. It is noted that the experimental load at a bond length of 100mm significantly exceeded the proportional value extrapolated from a bond length of 75mm, so this result could very likely be an experimental anomaly. If this were the case then the experimental effective bond length could be significantly higher than 100mm, hence much closer to the FEA value. The higher effective bond length obtained from the FE model may also be due to the fact that some imperfections in the testing samples were not considered in the model, such as the misalignment of steel plates. As a result of this, a larger bending moment could be presented causing a reduction in effective bond length (Phan et al., 2015).

Table 14. Experimental and FE results comparison

	Bond length (mm)	Ultimate load (kN) (experiment) (Phan et al., 2015) (1)	Ultimate load (FEA) (kN) (2)	Ratio (2/1)
Mild steel	75	70.0	71.9	1.03
	100	89.2	92.7	1.04
	125	90.1	104.6	1.16
High strength steel	75	77.5	82.7	1.07
	100	118.5	107.6	0.91
	125	119.0	125.5	1.05

The ultimate loads obtained by FE model are plotted in Figure 42 together with the experimentally obtained values reported in (Phan et al., 2015).The ratios of the ultimate loads of samples obtained in the FE model and the experiment are plotted in Figure 43. It can be seen that the FE results are consistently only about 5% higher, which could be attributed to assumed material properties. Some variation is easily explained by experimental uncertainty, and in particular the 100mm bond length result mentioned above is likely to be anomalous. In general the agreement is excellent considering these uncertainties, which suggests that the cohesive zone model works very well and could give very accurate results for the load carrying capacity of double strap joints with some calibration.

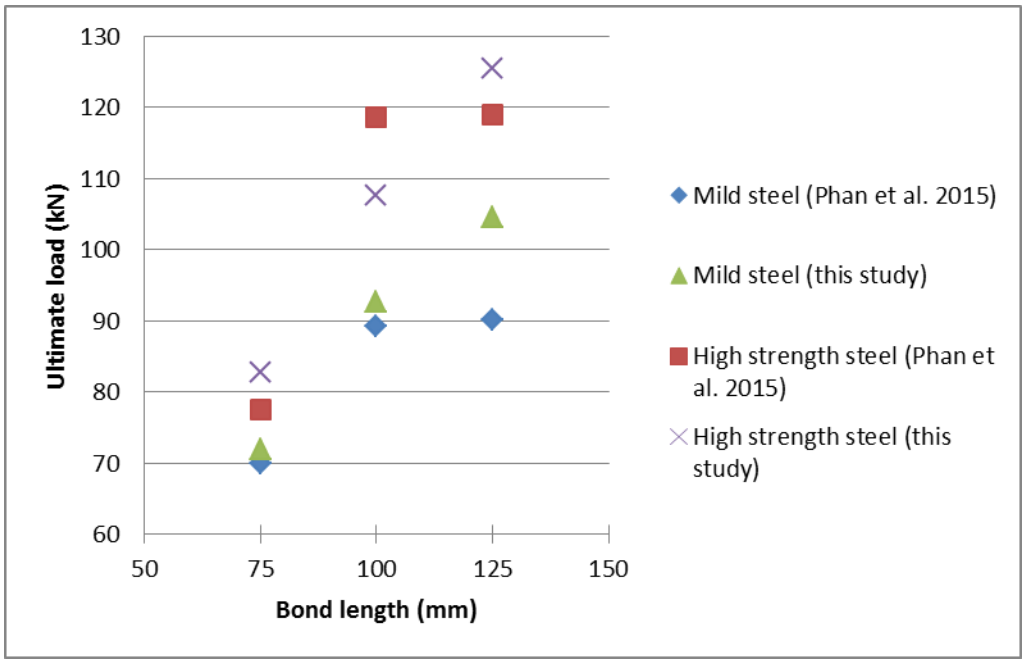

Figure 42. Ultimate load comparison between FE model and experiment

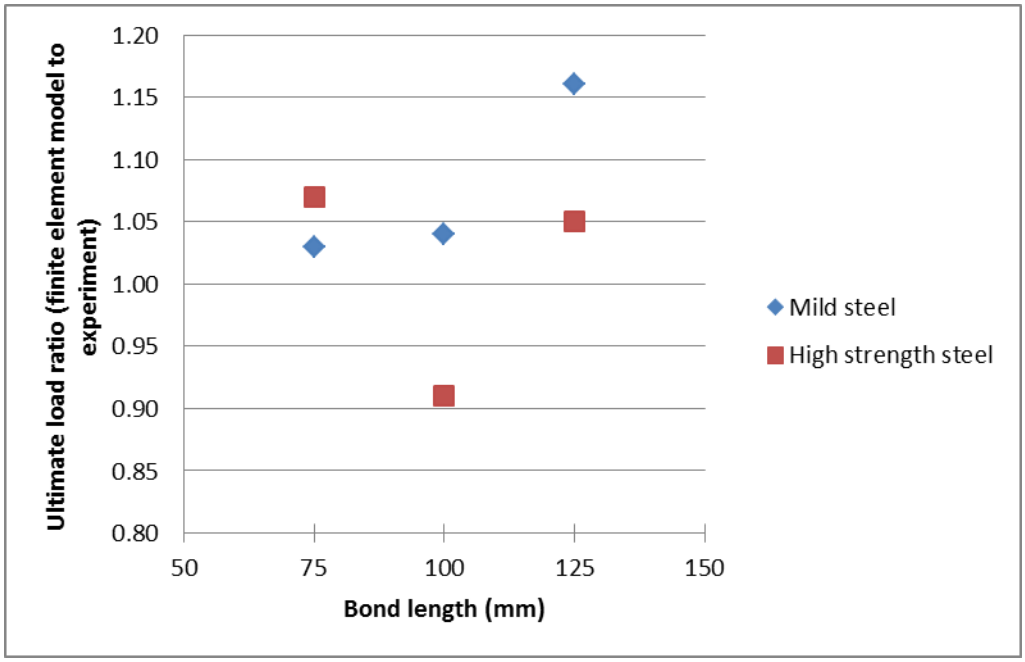

Figure 43. Ultimate load ratio versus bond length

6.3.3. Stress transfer and strain distribution along the bond length

A typical stress distribution in the sample and the final failure state are plotted in Figure 44(a) and (b) respectively. It can be seen that the stress was the highest at the joint and reduced at locations away from the joint. It was noted that the maximum stress in the CFRP was higher than the maximum stress in the steel due to the smaller cross-sectional dimension of the CFRP. Figure 44(b) shows the sample after failure. Note that since the model is displacement controlled, there is no load at failure, hence no stress, but the left end of the CFRP layer has displaced to the right after debonding, and similarly the right end of the steel layer has displaced to the left.

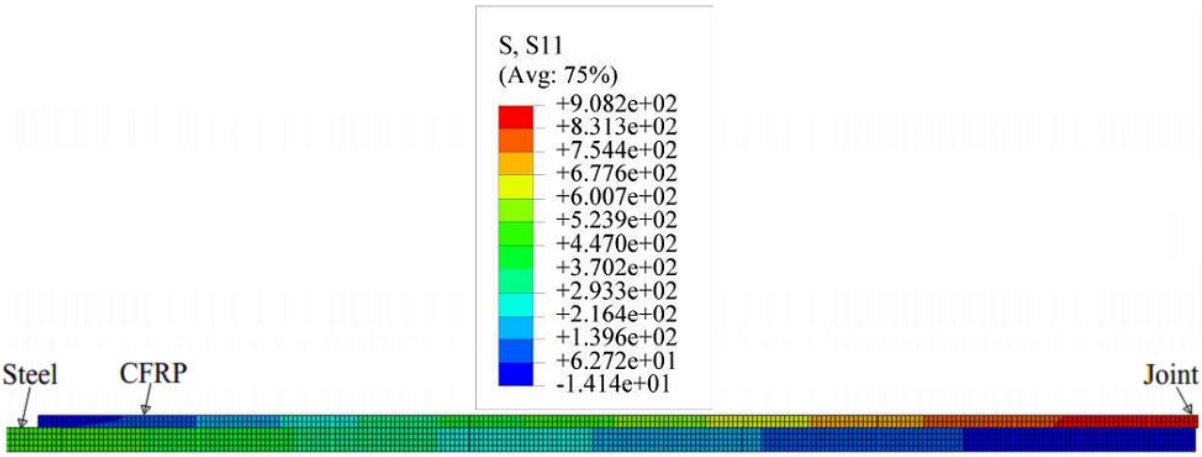

(a)

(b)

Figure 44. Stress transfer at 102.8kN (a) and debonding after failure (b)

Figure 45(a) and (b) compare the strain distributions in the CFRP of the high strength steel sample with 125mm bond length obtained respectively by the FE model and in experiment (Phan et al., 2015). It can be seen that the overall trend of the strain in the CFRP was similar for both Figure 45 (a) and (b), that is (i) the strain was greatest at 0mm (at the joint) where the CFRP carried the full load; (ii) the strain was very small at 120mm where the steel carried the majority of the load, and the effect of local debonding at the end of the CFRP layer starts to become apparent long before the full load is reached; and (iii) for low to moderately high loads the strain was essentially independent of position over most of the length of the bond away from either end, indicating that the load was fully shared between the CFRP and steel layers.

There was a transitional location where the strain or stress behaved differently as the load was increased. At higher load, the strain in the CFRP layer increased significantly in an expanding region near the joint, with a corresponding decrease in the steel layer (Figure 46), but remained unchanged in the remainder of the specimen, indicating a significant relative shear displacement that started at the joint and gradually progressed further into the specimen as the load was increased. This differs from full debonding because clearly some load is still carried by the steel. This transitional region varied and depended on the bond length, but for a bond length equal to or less than the effective bond length, this location was found to be about 80% of the bond length measured from the joint, e.g. 100mm in Figure 45(a). Otherwise it was 80% of the effective bond length (measure from the joint).

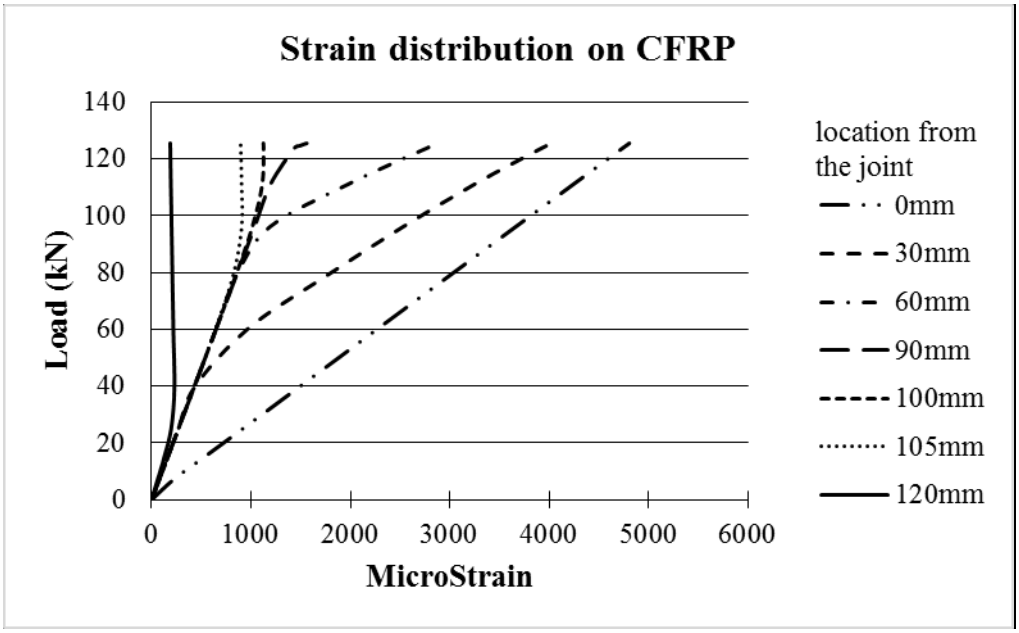

(a)

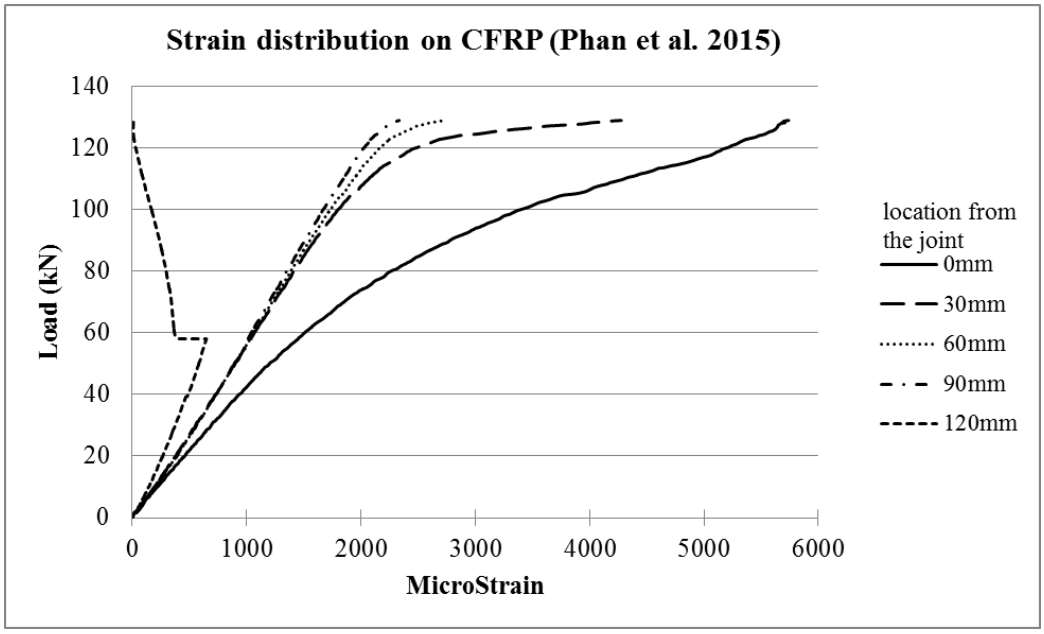

(b)

Figure 45. Strain distribution on CFRP at different locations (high strength steel with 125mm bond length) (a) FE model and (b) experimental results (Phan et al., 2015)

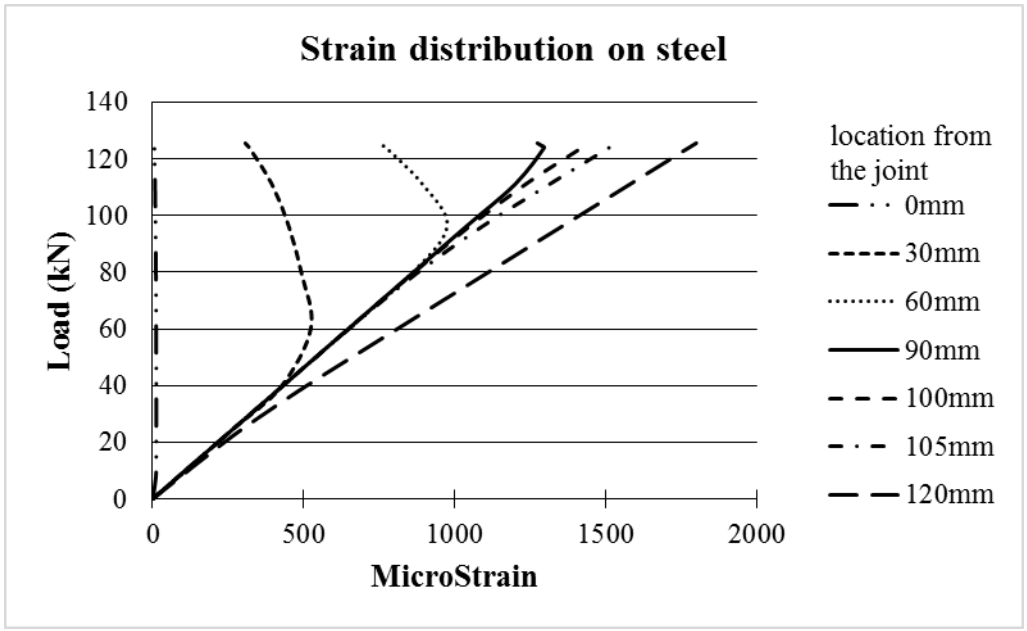

Figure 46. Strain distribution on steel at different locations (high strength steel with 125mm bond length)

As expected, the strain distributions in the CFRP and steel at the same locations (Figure 45 and Figure 46) show opposite trends, indicating transfer of the load between these layers. The strain in the steel was approximately zero at the joint but increased significantly towards the

bond end. However, after increasing to a certain value, it started to reduce when the load was increased. This phenomenon occurred only at the locations between 0mm and the transitional point.

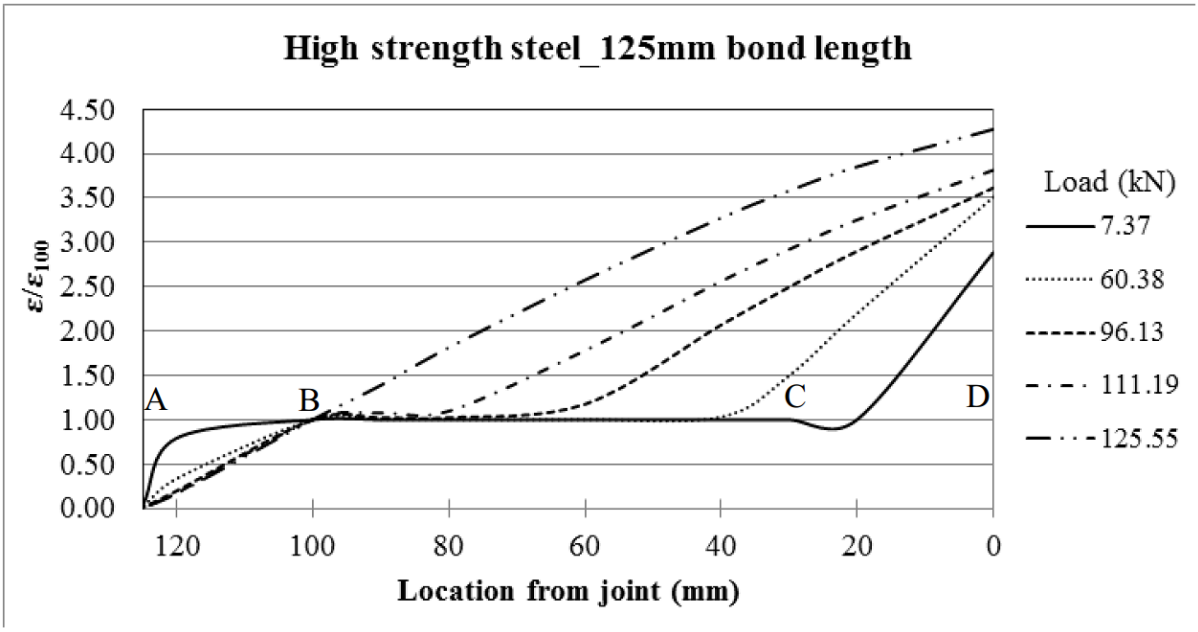

Figure 47. Strain ratio of different loads

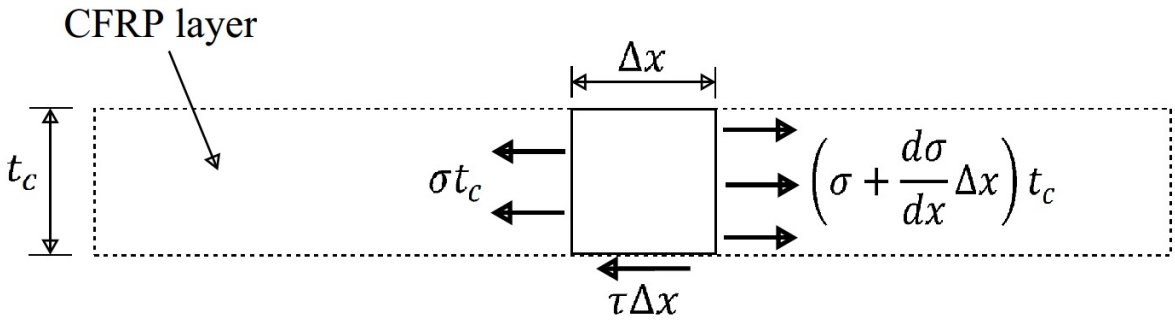

Figure 48. Equilibrium forces diagram

Figure 47 shows the ratio between normal strain at any location along the bond length and the strain at the transitional location. As shown in Figure 48, theoretical formulations were developed based on the testing results, i.e. the graph in Figure 46:

$$\tau \Delta x = \frac{d\sigma}{dx} \Delta x t_c \qquad (5)$$

$$hence \quad \tau = E_c t_c \frac{d\varepsilon}{dx} \qquad (6)$$

where E_c and t_c are Young's modulus and thickness of the CFRP, respectively.

The equilibrium requires that any change in normal strain (or stress) must be accompanied by a shear stress along the bond of $\tau = Et\varepsilon_{100}\frac{d\left(\frac{\varepsilon}{\varepsilon_{100}}\right)}{dx}$, which is the mechanism for transfer of load between the CFRP and steel layers. The slope in Figure 47 therefore represents the shear stress that could present between the CFRP and steel. When the ratio $\varepsilon/\varepsilon_{100} = 1$ it is essentially constant so no shear stress is present. At low load (7.37kN) shear stress occurs in regions AB and CD but it is small along AB, except at point A itself, and larger at CD. As the load increases the region with no shear stress becomes smaller. Finally, when the ultimate load is reached the shear stress presents over the entire bond length causing failure to occur.

6.4. Conclusion

Based on the numerical and FEA results, the following conclusions are drawn:

- The yield load of steel affects strongly the load carrying capacity of double strap joints. When the steel yields, failure occurred in the adhesive layer because of the large relative displacements between the layers being bonded irrespective of a higher bonding property of the epoxy resin.
- On one hand, mild steel samples failed with ductile failure while high strength steel samples fail mainly with brittle failure. On the other hand, with the same bond length, high strength steel sample could carry more loads due to the different properties of steel.
- The effective bond length is not unique when using various types of material. Larger bond length should be used for double strap joint with high strength steel. In this case, adhesive properties play an important role to decide the bond capacity.

- The finite element results agreed well with the experimental results, indicating that the cohesive zone model is adaptable to predict the ultimate load of the double strap joints. In particular it is able to predict whether the failure is ductile or not, which may result in material savings.
- The strain distribution was not uniform within the CFRP. There was a transitional location at about 80% of the bond length (or effective bond length) measured from the joint. At this location the strain in the CFRP started to behave differently, which helped to define the presence of the shear stress between CFRP and steel

Chapter 7. SUMMARY AND CONCLUSIONS

The primary objective of this research was the bond behaviour of CFRP and steel joint under various conditions and parameters. First, a series of experiments were carried out to determine the effective bond length of the samples based on the ultimate loads and the failure modes. The effective bond length was the maximum length that had significant effect to the bond strength. Any increment in bond length beyond this threshold value would not help increasing the ultimate load of the samples. The next stage was a series of tests aimed to investigate the effects of material properties on the bond behaviour of the joints, mainly based on the ultimate load and the failure modes. These various parameters included the adhesive properties, the steel yield strength, the CFRP types and the surface roughness. Thirdly, CFRP-to-steel joints were tested under fatigue loading in order to determine (a) the effect of primer resin on the fatigue life and (b) the effects of high and medium CFRP strand sheets on the performance of the samples under fatigue loading. Finally, a finite element model was established to compare the results with some obtained in the experiment. The following conclusions are made based on this study.

- For mild steel, the effective bond length was found to be approximately 100mm regardless to the utilisation of different adhesives and CFRP materials. Care must be taken during the installation process in order to obtain optimal outcomes. Any flaw in the preparation process such as lots of air bubbles between the fibres or contaminant on the bonding surface can cause a significant reduction in effective bond length. The finite element results confirmed that the effective bond length matched with that found in the experiments. However, the effective bond length is not unique when using various types of steel. Larger bond length should be used for double strap joint with high strength steel. With the same bond length, high strength steel sample could carry more loads due to the different properties of steel. A higher load capacity can be

obtained using the combination of high strength steel and CFRP plates if the joint is not the limiting factor. Strand CFRP sheets are not recommended for high strength steel since the ultimate loads were much lower than for those specimens prepared with CFRP plates.

- Three different failure modes were found in this study depending on the uses of CFRP adhesive types. There was no clear evidence that demonstrated the relationship between the failure modes and the ultimate loads. It was due to some other factors such as the steel yield load which affects strongly the load carrying capacity of double strap joints. When the steel yields, failure occurred in the adhesive layer (causing adhesion failure) because of the large relative displacements between the layers being bonded irrespective of a higher bonding property of the epoxy resin. In order to obtain the highest ultimate load, CFRP plates are recommended for all flat surfaces due to the fact that the application process is much simpler and therefore minimise the flaws that can take place.
- It was found that the surface preparation process can be done with either grinding discs or sand blasting depending on the available tools. It should be noted that the bonding surface roughness should not be too large to avoid difficulty in the following process. The ideal surface roughness of about 2.95μm is recommended regardless to the techniques used.
- CFRP strand sheet is particularly suitable for steel joints under fatigue loading. Some traditional steps can be eliminated such as the use of rollers and vacuum bags, and the fatigue lives are comparable to those obtained with other types of CFRP. Two or more layers of CFRP strand sheets are recommended to avoid CFRP rupture. Primer resin is not recommended since it caused a linear reduction in fatigue life with the increase of

the stress range. More tests with different primer resins are needed to find a more suitable primer resin.

REFERENCE

Abaqus 2013. ABAQUS Theory manual and user's manual. Providence, RI, USA: Dassault Systemes Simulia Corp.

Al-Zubaidy, H., Al-Mahaidi, R. & Zhao, X.-L. 2013. Finite element modelling of CFRP/steel double strap joints subjected to dynamic tensile loadings. *Composite Structures,* 99**,** 48-61.

Athawale, P. 2012. *Analysis of factors affecting effective bond length for fiber reinforced polymer composite laminate externally bonded to concrete substrate.* Master of science in Civil Engineering, Texas Tech University.

Baldan, A. 2004. Adhesively-bonded joints and repairs in metallic alloys, polymers and composite materials: Adhesives, adhesion theories and surface pretreatment. *Journal of Materials Science,* 39**,** 1-49.

Barbero, E. J. 2013. *Finite element analysis of composite materials with Abaqus*.

Ben Ouezdou, M., Bae, S. & Belarbi, A. 2008. Effective bond length of externally bonded FRP sheets. *Fourth International Conference on FRP Composites in Civil Engineering (CICE2008).* Zurich, Switzerland.

Bocciarelli, M. & Colombi, P. 2012. Elasto-plastic debonding strength of tensile steel/CFRP joints. *Engineering Fracture Mechanics,* 85**,** 59-72.

Bocciarelli, M., Colombi, P., Fava, G. & Poggi, C. 2009. Fatigue performance of tensile steel members strengthened with CFRP plates. *Composite Structures,* 87**,** 334-343.

Chataigner, S., Gagnon, A., Quiertant, M., Benzarti, K. & Aubagnac, C. 2012. Adhesively bonded composite reinforcements for steel structures: durability of the stress transfer. *CICE 2012, International Conference on FRP Composites in Civil Engineering.* ROME.

Colombi, P. & Fava, G. 2012. Fatigue behaviour of tensile steel/CFRP joints. *Composite Structures,* 94**,** 2407-2417.

Da Silva, L. F. M. & Campilho, R. D. S. G. 2012. Advances in Numerical Modelling of Adhesive Joints. *Advances in Numerical Modeling of Adhesive Joints.* Springer Berlin Heidelberg.

Dawood, M. & Rizkalla, S. 2010. Environmental durability of a CFRP system for strengthening steel structures. *Construction and Building Materials,* 24**,** 1682-1689.

Dehghani, E., Daneshjoo, F., Aghakouchak, A. A. & Khaji, N. 2012. A new bond-slip model for adhesive in CFRP-steel composite systems. *Engineering Structures,* 34**,** 447-454.

El Damatty, A. A. & Abushagur, M. 2003. Testing and modeling of shear and peel behavior for bonded steel/FRP connections. *Thin-Walled Structures,* 41**,** 987-1003.

Fawzia, S. & Karim, A. 2009. Investigation into the bond between CFRP and steel plates. *In:* Ardil, C. (ed.) *The World Academy of Science, Engineering and Technology.* Tokyo, Japan.

Fawzia, S., Zhao, X.-L., Al-Mahaidi, R. & Rizkalla, S. 2005a. Double strap joint tests to determine the bond characteristics between CFRP and steel plates. *the Fourth International Conference on Advances in Steel Structures.* Shanghai, China.

Fawzia, S., Zhao, X. L., Al-Mahaidi, R. & Rizkalla, S. 2005b. Bond characteristics between CFRP and steel plates in double strap joints. *Advanced Steel Construction - An International Journal,* 1**,** 17-28.

Fernando, D. 2010. *Bond behaviour and debonding failures in CFRP-strengthened steel members.* Ph.D, The Hong Kong Polytechnic University.

Fernando, D., Teng, J. G., Yu, T. & Zhao, X. L. 2013. Preparation and characterization of steel surfaces for adhesive bonding. *Journal of Composites for Construction,* 17.

Fernando, D., Yu, T. & Teng, J. G. 2014. Behavior of CFRP Laminates Bonded to a Steel Substrate Using a Ductile Adhesive. *Journal of Composites for Construction,* 18**,** 04013040.

Francis, R. 1982. *Guides to good practice in corrosion control* [Online]. National Physical Laboratory, Teddington, Middlesex TW11 0LW. Available: http://www.npl.co.uk/upload/pdf/bimetallic_20071105114556.pdf [Accessed 23rd October 2014].

Gorss, J. 2003. *High performance carbon fibers.* *http://www.acs.org/content/acs/en/education/whatischemistry/landmarks/carbonfibers.html* [Online]. American Chemical Society September 2014].

Harris, A. F. & Beevers, A. 1999. The effects of grit-blasting on surface properties for adhesion. *International Journal of Adhesion and Adhesives,* 19**,** 445-452.

Hegde, R. R., Dahiya, A. & Kamath, M. G. 2004. *Carbon fibres* [Online]. Materials science & engineering 554 - nonwovens science and technology II.

Hidekuma, Y., Kobayashi, A. & Komori, A. 2013. Tensile test of CFRP bonded steel plate with heat resistance epoxy resin. *Fourth Asia-Pacific Conference on FRP in Structures (APFIS 2013).* Melbourne, Australia.

Hidekuma, Y., Kobayashi, A., Miyashita, T. & Nagai, M. 2011. Reinforcing effect of CFRP strand sheets on steel members. *Journal of Physical Science and Application,* 1(3)**,** 155-162.

Hidekuma, Y., Kobayashi, A., Okuyama, Y., Miyashita, T. & Nagai, M. 2012. Experimental study on debonding behavior of CFRP for axial tensile reinforced steel plate by CFRP strand sheets. *The Third Asia-Pacific Conference on FRP in Structures (APFIS2012).*

Hollaway, L. C. & Cadei, J. 2002. Progress in the technique of upgrading metallic structures with advanced polymer composites. *Progress in Structural Engineering and Materials,* 4**,** 131-148.

Jahn, B. 2013. Composites market report 2013: Market developments, trends, challenges and oppotunities. AVK Industrievereinigung, Federation of Reinforced Plastics.

Jiao, H., Mashiri, F. R. & Zhao, X. L. 2012a. A Comparative Study on Fatigue Behaviour of Steel Beams Retrofitted with Welding, Pultruded CFRP Plates and Wet Layup CFRP Sheets. *Thin-Walled Structures,* 59**,** 144-152.

Jiao, H., Phan, H. B. & Zhao, X.-L. 2014. Fatigue behaviour of Steel elements strengthened with strand CFRP sheets. *Advances in Structural Engineering,* 17**,** 1719-1727.

Jiao, H., Phan, H. B. & Zhao, X. L. 2012b. Fatigue testing of defected steel beams retrofitted using sandwich-layered high and normal modulus CFRP sheets. *6th International Composites Conference.* Monash University, Melbourne, Australia.

Jiao, H., Phan, H. B. & Zhao, X. L. 2012c. Fatigue testing of defected steel beams retrofitted using sandwich-layered high and normal modulus CFRP sheets. *ACUN6 –Composites and Nanocomposites in Civil, Offshore and Mining Infrastructure, Melbourne 14 – 16 November 2012***,** 1-6.

Jiao, H. & Zhao, X.-L. 2004a. CFRP strengthened butt-welded very high strength (VHS) circular steel tubes. *Thin-Walled Structures,* 42**,** 963-978.

Jiao, H. & Zhao, X. L. 2004b. CFRP strengthened butt-welded very high strength (VHS) circular steel tubes. *Thin-Walled Structures,* 42**,** 963-978.

Jiao, H. & Zhao, X. L. 2008. Simulation of CFRP strengthened butt-welded very high strength (VHS) circular steel tubes in tension. *12th International Symposium on Tubular Structures (ISTS12).* Shanghai.

Jiao, H., Zhao, X. L., Kobayashi, A. & Wood, D. 2013. Fatigue testing of defected steel beams repaired using medium and high modulus CFRP strand sheets. *Fourth Asia-Pacific Conference on FRP in Structures (APFIS 2013).* Melbourne, Australia.

Jiao, H., Zhao, X. L. & Mashiri, F. R. 2012d. Improving Fatigue Performance of CFRP Strengthened Steel Beams by Applying Vacuum Pressure in the Wet Layup of CFRP Woven Sheets. *The Third Asia-Pacific Conference on FRP in Structures.* Hokkaido University, Japan: Accepted.

Jis 2004. Test method for tensile properties of fiber reinforced polymer (FRP) sheets for reinforcement of concrete, JIA A 1191. *Japanese Industrial Standard*.

Julian, E. & Jofre, L. 2013. *Durability of Adhesively-Bonded CFRP/Steel Joints - Modelling of moisture ingress and joint degradation.* Master, Chalmers University of Technology.

Kraus, T. & Kuhnel, M. 2014. Composites market report: Market developments, trends, challenges and oppotunities. AVK Industrievereinigung, Federation of Reinforced Plastics.

Lam, C. C. 2009. *Finite element study of bond-slip nehaviour of CFRP and GFRP laminates on brick masonry.* Masters, University of Padova.

Liu, H. B., Zhao, X. L. & Al-Mahaidi, R. The effect of fatigue loading on bond strength of CFRP bonded steel plate joints. *In:* Teng, C. A., ed. Proceedings of the International Symposium on Bond Behaviour of FRP in Structures (BBFS 2005), International Institute for FRP in Construction, 2005 Hong Kong, China. 451-456.

Liu, H. B., Zhao, X. L. & Al-Mahaidi, R. 2010. Effect of fatigue loading on bond strength between CFRP sheets and steel plates. *International Journal of Structureal Stability and Dynamics,* 10**,** 1-20.

Luke, S. & Consulting, M. 2001. The Use of Carbon Fibre Plates for the Strengthening of Two Metallic Bridges of a Historic Nature in the UK. *In:* Teng, J.-G. (ed.) *FRP Composites in Civil Engineering.* Hong Kong, China: Amsterdam; New York: Elsevier.

Mays, G. C. & Hutchinson, A. R. 1992. *Adhesives in civil engineering,* New York, Cambridge University Press.

Mertz, D. R., Gillespie, J. W., Chajes, M. J. & Sabo, S. A. 2002. The Rehabilitation of Steel Bridge Girders Using Advanced Composite Materials. NCHRP-IDEA Project 51.

Miller, T., Chajes, M., Mertz, D. & Hastings, J. 2001. Strengthening of a Steel Bridge Girder Using CFRP Plates. *Journal of Bridge Engineering,* 6**,** 514-522.

Mitchell, R. A., Woolley, R. M. & Chwirut, D. J. 1975. Analysis of Composite-Reinforced Cutouts and Cracks. *AIAA Journal,* 13**,** 744-749.

Nakazawa, M. 1994. Mechanism of adhesion of epoxy resin to steel surface. Nippon steel technical report.

Nguyen, T. C., Bai, Y., Zhao, X. L. & Al-Mahaidi, R. 2011. Mechanical characterization of steel/CFRP double strap joints at elevated temperatures. *Composite Structures,* 93**,** 1604-1612.

Nguyen, T. C., Bai, Y., Zhao, X. L. & Al-Mahaidi, R. 2012. Durability of steel/CFRP double strap joints exposed to sea water, cyclic temperature and humidity. *Composite Structures,* 94**,** 1834-1845.

Nozaka, K., Shield, C. K. & Hajjar, J. F. 2005. Design of a Test Specimen to Assess the Effective Bond Length of Carbon Fiber-Reinforced Polymer Strips Bonded to Fatigued Steel Bridge Girders. *Journal of composites for construction,* 9**,** 304-312.

Packham, D. E. 2003. Surface energy, surface topography and adhesion. *International Journal of Adhesion and Adhesives,* 23**,** 437-448.

Parvin, A. & Brighton, D. 2014. FRP Composites Strengthening of Concrete Columns under Various Loading Conditions. *Polymers (20734360),* 6**,** 1040-1056.

Phan, H. B., Holloway, D. S. & Jiao, H. 2015. An investigation into the effect of roughness conditions and materials on bond strength of CFRP/steel double strap joints (accepted for publication). *Australian Journal of Structural Engineering*.

Poorna Chander, K., Vashista, M., Sabiruddin, K., Paul, S. & Bandyopadhyay, P. P. 2009. Effects of grit blasting on surface properties of steel substrates. *Materials & Design,* 30**,** 2895-2902.

Ratwani, M. M. 1977. Characterization of fatigue crack growth in bonded structures. Volumn I: crack growth prediction in bonded structures. Northrop Corporation, Aircraft Division, Hawthorne, California.

Saa 1991. Methods for tensile testing of metals. *Australian Standard AS1391,* Sydney.

Saa 2002. AS 3572.7-2002 : Plastics - Glass filament reinforced plastics (GRP) - Methods of test - Determination of extension to failure of unreinforced resins. *Australian standard*.

Schnerch, D. 2005. *Strengthening steel structures and bridges with high modulus carbon fiber reinforced polymers.* PhD.

Schnerch, D., Dawood, M., Rizkalla, S. & Sumner, E. 2007. Proposed design guidelines for strengthening of steel bridges with FRP materials. *Construction and Building Materials,* 21**,** 1001-1010.

Sykes, J. M. 1982. *Surface treatments for steel,* Applied Science Publishers, London, UK.

Tabrizi, S., Rizkalla, S. & Kobayashi, A. CFRP strands for flexural strengthening of steel bridges. Fourth Asia-Pacific Conference on FRP in Structures (APFIS 2013), 11-13 December 2013, 2013 Melbourne, Australia.

Talreja, R. 1981. Fatigue of Composite Materials: Damage Mechanisms and Fatigue-Life Diagrams. *Proceedings of the Royal Society of London. Series A, Mathematical and Physical Sciences,* 378**,** 461-475.

Tamai, Y. & Aratani, K. 1972. Experimental study of the relation between contact angle and surface roughness. *The Journal of Physical Chemistry,* 76**,** 3267-3271.

Tavakkolizadeh, M. & Saadatmanesh, H. 2001. Galvanic corrosion of carbon and steel in aggressive environments. *Journal of Composites for Construction,* 5**,** 200-210.

Taylor, C., Jiao, H., Phan, H. B. & Zhao, X.-L. Bond Strength of Steel plates Connected using Strand CFRP Sheets and Selected Epoxy Resins. The 7th International Conference on FRP Composites in Civil Engineering, International Institute for FRP in Construction, 2014 Vancouver, Canada.

Taylor, C., Jiao, H., Zhao, X. & Kobayashi, A. Debonding strength of steel joints strengthened using Strand CFRP sheets under axial tension. APFIS2013, Melbourne, 11-13 December 2013, 2013.

Teng, J. G., F., C. J., T., S. S. & L., L. 2001. *FRP–strengthened RC structures,* West Sussex, PO19 1 UD, England, John Wiley & Sons, Ltd.

Teng, J. G., Fernando, D., Yu, T. & Zhao, X. L. 2010. Treatment of steel surfaces for effective adhesive bonding. *Fifth International Conference on FRP Composites in Civil Engineering, CICE-2010.* Beijing, China.

Teng, J. G., Fernando, D., Yu, T. & Zhao, X. L. 2012a. Debonding Failures in CFRP-Strengthened Steel Structures. *APFIS2012, 2-4 Feb 2012.* Japan.

Teng, J. G., Yu, T. & Fernando, D. 2012b. Strengthening of steel structures with fiber-reinforced polymer composites. *Journal of Constructional Steel Research,* 78**,** 131-143.

Volnyy, V. A. & Pantelides, C. P. 1999. Bond Length of CFRP Composites Attached to Precast Concrete Walls. *Journal of Composites for Construction,* 3**,** 168.

Wu, C., Zhao, X.-L., Al-Mahaidi, R. & Duan, W. 2010. Experimental Study on Bond Behaviour between UHM CFRP Laminate and Steel. *In:* Ye, L., Feng, P. & Yue, Q. (eds.) *The 5th International Conference on FRP Composites in Civil Engineering (CICE 2010).* Beijing, China.

Wu, C., Zhao, X., Hui Duan, W. & Al-Mahaidi, R. 2012a. Bond characteristics between ultra high modulus CFRP laminates and steel. *Thin-Walled Structures,* 51**,** 147-157.

Wu, C., Zhao, X. L., Chiu, W. K., Al-Mahaidi, R. & Duan, W. H. Bond behaviour between UHM CFRP plate and steel plate under fatigue loading. 6th International Conference on FRP Composites in Civil Engineering (CICE 2012), Rome, Italy, 13-15 June 2012, 2012 2012b. 1-8.

Wu, C., Zhao, X. L., Chiu, W. K., Al-Mahaidi, R. & Duan, W. H. 2012c. Bond behaviour between UHM CFRP plate and steel plate under fatigue loading. *The 6th International Conference on FRP Composites in Civil Engineering (CICE 2012).* Rome, Italy: International Institute for FRP in Construction.

Wu, C., Zhao, X. L., Chiu, W. K., Al-Mahaidi, R. & Duan, W. H. 2013. Effect of fatigue loading on the bond behaviour between UHM CFRP plates and steel plates. *Composites Part B: Engineering,* 50**,** 344-353.

Xia, S. H. & Teng, J. G. 2005. Behaviour of FRP-to-steel bonded joints. *International Symposium on Bond Behaviour of FRP in Structures (BBFS).* Hong Kong, China.

Yu, T., Fernando, D., Teng, J. G. & Zhao, X. L. 2012. Experimental study on CFRP-to-steel bonded interfaces. *Composites Part B-Engineering,* 43**,** 2279-2289.

Zhao, X.-L. & Zhang, L. 2007. State-of-the-art review on FRP strengthened steel structures. *Engineering Structures,* 29**,** 1808-1823.